Early Pleistocene initiation of the San Felipe fault zone, SW Salton Trough, during reorganization of the San Andreas fault system

Alexander N. Steely*
Susanne U. Janecke†
Department of Geology, Utah State University, Logan, Utah 84322-4505

Rebecca J. Dorsey
Department of Geological Sciences, University of Oregon, Eugene, Oregon 97405, USA

Gary J. Axen
Department of Earth and Environmental Science, New Mexico Institute of Mining and Technology, Socorro, New Mexico 87801, USA

ABSTRACT

Structural and stratigraphic analyses along the western margin of the Salton Trough show that the San Andreas fault system was reorganized in early Pleistocene time from a system dominated by two fault zones (the San Andreas fault and the West Salton detachment fault) to a network of dextral faults that include the San Andreas and at least four dextral faults to the southwest. The San Felipe fault zone, one of these dextral faults, has ~5.8 ± 2.8 km of right separation and consists of three principal faults in the Peninsular Ranges. These are the San Felipe fault in the WNW, Sunset fault in the middle, and Fish Creek Mountains fault in the ESE. They form a left-stepping array and bound domains in which the Sunset Conglomerate, the older West Salton detachment fault, and Cretaceous mylonitic rocks below the detachment are folded about WNW-trending folds. A complex flower structure within the left-stepovers probably produced this fault-parallel folding. Because all the rocks within stepovers of the San Felipe fault zone, from Cretaceous to Pleistocene, are deformed about WNW-trending folds and record broadly similar shortening strains, we infer a Quaternary age of deformation. Parts of the San Felipe fault zone cut latest Pleistocene to Holocene surficial deposits, and the fault zone is likely active.

Evidence for early Pleistocene initiation of the San Felipe fault zone is preserved in conglomerate NE of the Sunset fault. Poorly sorted angular boulder conglomerate and pebbly sandstone of the Sunset Conglomerate are ~600 m thick and lie in angular unconformity on the Pliocene Palm Spring Group. The conglomerate coarsens upward and toward the fault, and is dominated by plutonic clasts derived from SW of it. Conglomerate beds contain up to 10% sandstone clasts recycled from older basin fill and accumulated in proximal to medial alluvial fans that were shed to the NE from uplifted rocks along the then-active Sunset fault.

Based on lithologic, stratigraphic, structural, and compositional similarities, we correlate the Sunset Conglomerate to the Pleistocene Ocotillo Formation. Clasts of recycled sandstone record erosion of detachment-related basin fill that predates the San Felipe fault and once covered the Vallecito and Fish Creek mountains. These crystalline-cored mountain ranges first emerged from beneath basin fill during early slip above the nascent San Felipe fault ca. 1.1–1.3 Ma. Later, the San Felipe fault zone cut upward, folded, cut across, and deactivated the West Salton detachment fault within a ~9-km-wide contractional bend and pair of left-steps. Areas that accumulated sediment within this stepover zone between ca. 1.1 and ca. 0.6 Ma are currently being inverted and folded.

Initiation of the San Felipe fault in early Pleistocene time was a significant event in the reorganization of the southern San Andreas fault system. The Quaternary dextral faults broadened the plate boundary zone southwestward from roughly 25 km (during coeval slip on the San Andreas fault and West Salton detachment fault) to 50–70 km, and mark a change in the dominant structural style from transtension to distributed dextral faulting south of the Big Bend.

Keywords: strike-slip fault, Ocotillo Formation, contractional step, reorganization, detachment fault.

INTRODUCTION

Rocks and structures in the Salton Trough contain a record of complex late Cenozoic deformation and sedimentation related to the evolution of the Pacific–North America plate boundary in southern California and northern Mexico (Fig. 1) (Dibblee, 1954; Atwater, 1970; Sharp, 1972; Crowell, 1981; Winker, 1987; Winker and Kidwell, 1986, 1996; Axen and Fletcher, 1998; Dorsey, 2006; Steely, 2006). During late Miocene (?) and Pliocene time the West Salton detachment fault was a major structure that produced the Salton supradetachment basin in its hanging wall (Axen and Fletcher, 1998; Dorsey, 2006). The detachment probably continued to slip into the early Pleistocene based on the presence of lower Pleistocene conglomerate and megabreccia shed from its footwall (Axen and Fletcher, 1998; Winker and Kidwell, 2002; Dorsey and Janecke, 2002; Dorsey et al., 2006; Kairouz, 2005). Plate boundary strain during this time was divided between the master southern San Andreas fault and the secondary West Salton detachment fault (Axen and Fletcher, 1998). Beginning sometime in Pleistocene time, the relatively simple two-fault zone system was replaced by a more complex system in which roughly half of the strain was distributed unevenly across new dextral-oblique faults south of the Big Bend in the San Andreas fault (Morton and Matti, 1993). This incompletely

*E-mail: asteely@gmail.com
†E-mail: susanne.janecke@usu.edu

GSA Bulletin; May/June 2009; v. 121; no. 5/6; p. 663–687; doi: 10.1130/B26239.1; 15 figures; 1 table.

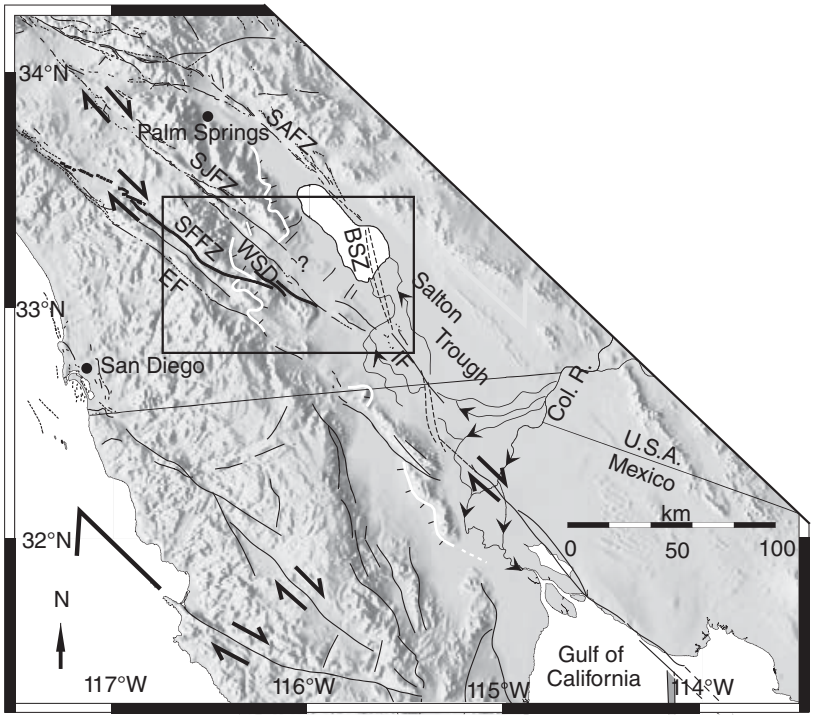

Figure 1. Tectonic overview of southern California and northern Mexico. San Felipe fault zone (SFFZ) is in bold black; other strike-slip faults are in black; SAFZ—San Andreas fault zone; SJFZ—San Jacinto fault zone; IF—Imperial fault; SJFZ—San Jacinto fault zone; EF—Elsinore fault; BSZ—Brawley Seismic Zone. Oblique-slip detachment faults are in white including the WSD—West Salton detachment fault. Fault locations are from Jennings (1977) and Axen and Fletcher (1998). Modified from Kirby et al. (2007). Box is approximate location of Figure 2.

understood event disrupted and deactivated most of the West Salton detachment fault, reorganized the San Andreas fault system, and after some additional modifications, resulted in the current fault system of southern California. The San Andreas, the San Jacinto, Elsinore, Earthquake Valley, and San Felipe fault zones are the principal Quaternary faults in this region (Figs. 1 and 2). Our focus is on the San Felipe fault zone in the center of the system of new faults.

This study seeks to answer several important questions: When did the San Felipe fault zone initiate SW of the San Andreas fault? Was there a temporal overlap between the nascent San Felipe fault zone and the older West Salton detachment fault? If so, what was the duration of coeval slip? Did the new dextral faults initiate simultaneously or diachronously? How did the San Felipe fault zone develop through time, what was its structural style, and did it accumulate enough slip to be classified as a moderate-sized dextral fault within the San Andreas fault system? Did initiation of the San Felipe fault zone reorganize the supradetachment basin that had formed in the Pliocene above the West Salton detachment fault, as Lutz et al. (2006) and Kirby et al. (2007) proposed? What was the basinal response to the growing San Felipe fault zone? Is the San Felipe fault zone currently inactive, as some have suggested? Answering these questions will lead to a better understanding of the major kinematic and structural change that occurred within the San Andreas fault system during the Pleistocene.

In this paper we integrate new data sets with previous magnetostratigraphic studies and basin and structural analysis in the western Salton Trough to document an oblique strike-slip fault zone that cut, folded, and deactivated the West Salton detachment fault during deposition of the syntectonic Ocotillo Formation along the SW margin of the newly formed San Felipe–Borrego subbasin (Housen et al., 2005; Lutz et al., 2006; Kirby et al., 2007). We first describe the regional setting, stratigraphic relationships, and the age of the San Felipe fault zone. We then examine and interpret structural geometries in the central contractional part of the fault zone, and integrate these interpretations into a broader regional context.

To better understand the timing and structural style of this major tectonic reorganization along the plate boundary, we characterize and date the transition from slip on the West Salton detachment fault to slip on the San Felipe fault zone in the western Salton Trough (Figs. 1 and 2). We examined exposures near Yaqui Ridge at the SW margin of the San Felipe–Borrego subbasin to constrain the stratigraphic and structural evolution of these structures (Fig. 3). Geologic mapping over an area of ~2.5 U.S. Geological Survey (USGS) 7.5′ quadrangles was carried out at scales of 1:12,000 and 1:24,000 in the Borrego Mountain, Borrego Sink, Harper Canyon, Whale Peak, and Squaw Peak 7.5′ USGS quadrangles (Steely, 2006). Stratigraphic, sedimentologic, and structural analyses reported here are condensed from Steely (2006).

Regional Geology

The San Felipe fault zone strikes WNW and is oriented ~10°–20° counterclockwise from the adjacent San Jacinto and Elsinore fault zones. It is a major dextral strike-slip fault that approaches the Elsinore fault zone in the WNW and projects toward the Superstition Mountain segment of the San Jacinto fault zone to the ESE (Dibblee, 1954; Rogers, 1965; Figs. 1 and 2). The San Felipe and Elsinore fault zones were previously inferred to have initiated by or before ca. 2 Ma in the Peninsular Ranges, with little significant slip since ca. 0.9 Ma (Lamar and Rockwell, 1986; Hull and Nicholson, 1992; Magistrale and Rockwell, 1996). However, recent work in the adjacent San Felipe Hills (Kirby, 2005; Kirby et al., 2007) and Borrego Badlands (Lutz, 2005; Lutz et al., 2006) documents a major stratigraphic and structural reorganization at ca. 1.1 Ma that is interpreted as initiation of the San Felipe fault in the early Pleistocene, not its demise. Because these studies examined basin fill in a distal position relative to the San Felipe fault zone, the ca. 1.1 Ma stratigraphic changes were linked to the basin-bounding San Felipe fault zone using indirect methods (Lutz et al., 2006; Kirby et al., 2007). This study examines deposits within and proximal to the San Felipe fault zone in order to assess its age of initiation and activity, and to determine if it is partially coeval with the West Salton detachment fault at Yaqui Ridge.

The adjacent San Jacinto fault zone strikes NW, is almost 300 km long, and merges with the Imperial fault in the SE and the San Andreas fault in the NW (Figs. 1 and 2) (Sharp, 1967; Sanders, 1989). Many previous studies of the San Jacinto fault zone show that it is an early Pleistocene-Recent fault with high slip rates that allow some plate motion to bypass the eastern

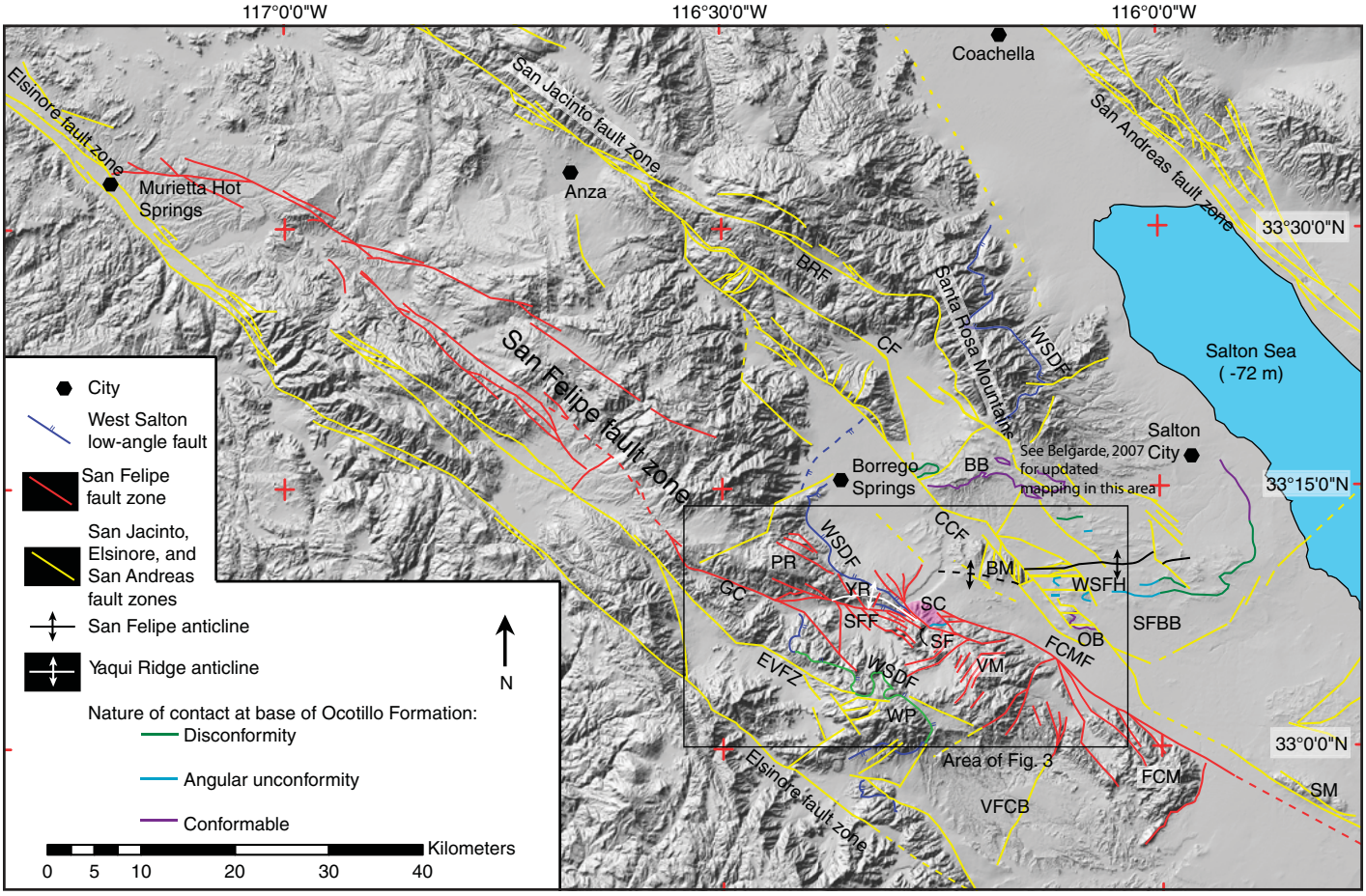

Figure 2. Important structural features of southern California and the nature of the basal contact of the Ocotillo Formation in the western Salton Trough. Faults of the San Felipe fault zone (SFFZ) are red. Note that the West Salton low-angle fault is folded and cut by dextral strike-slip fault zones at Yaqui Ridge. Light Green denotes a part of the West Salton detachment fault that is still active within the dextral fault system to the south. Faults are compiled and modified from Rogers (1965); Jennings (1977); Kennedy and Morton (1993); Kirby (2005); Lutz (2005); Kennedy (2000, 2003;) and this study. BB—Borrego Badlands; BM—Borrego Mountain; BRF—Buck Ridge fault; CCF—Coyote Creek fault; CF—Clark fault; EVFZ—Earthquake Valley fault zone; FCM—Fish Creek Mountains; FCMF—Fish Creek Mountains fault; GC—Grapevine Canyon; OB—Ocotillo Badlands; PR—Pinyon Ridge; SC—Sunset Conglomerate of the Ocotillo Formation (pink); SF—Sunset fault; SFF—San Felipe fault; SFBB—San Felipe-Borrego subbasin; SM—Superstition Mountain; VFCB—Vallecito–Fish Creek subbasin; VM—Vallecito Mountains; WP—Whale Peak; WSDF—West Salton detachment fault; WSFH—western San Felipe Hills; YR—Yaqui Ridge.

half of the Big Bend in the San Andreas fault (e.g., Sharp, 1967; Bartholomew, 1968; Rockwell et al., 1990; Matti and Morton, 1993; Morton and Matti, 1993; Bennett et al., 1996; Dorsey, 2002; Kendrick et al., 2005; Janecke et al., 2005b; Fialko, 2006; Lutz et al., 2006; Kirby et al., 2007). The San Jacinto, San Felipe, Earthquake Valley, and Elsinore dextral strike-slip fault zones cut obliquely across the western Salton Trough, are currently active, and deform late Pleistocene and/or Holocene deposits (Rockwell et al., 1990; Hull and Nicholson, 1992; Morton and Matti, 1993; Dorsey, 2002; Kirby, 2005; Lutz et al., 2006; Belgarde, 2007; this study).

Most of the West Salton detachment fault zone has been or is being uplifted and exhumed between and adjacent to younger dextral faults (Axen and Fletcher, 1998; Kairouz, 2005; Matti et al., 2006; Steely, 2006; Belgarde, 2007). Only one or two short segments of the detachment fault continue to slip in an area north of Whale Peak, where younger crosscutting dextral strike-slip faults may be activating patches of the preexisting detachment fault (Figs. 2 and 3) (Kairouz, 2005; Steely, 2006). The West Salton detachment fault partly reactivated the Eastern Peninsular Ranges mylonite zone. This mid- to late-Cretaceous, west-directed, reverse- to thrust-sense shear zone underlies all but the southernmost part of the West Salton detachment fault (Schultejann, 1984; Lough, 1993; Axen and Fletcher, 1998; Steely, 2006). The West Salton detachment fault and mylonite generally strike NNW and dip ENE, but both vary in their strike and locally even in their dip direction (Axen and Fletcher, 1998; Kairouz, 2005; Steely, 2006). We use the regional ENE dip-direction of the >125-km-long detachment fault and mylonite zone as reference directions for structural analysis.

Some original variation in the strike of the mylonite and detachment fault is possible in the study area at Yaqui Ridge and elsewhere along the detachment fault (Steely, 2006). Adjacent to the San Felipe–Borrego subbasin there are many changes in strike, and locally even the dip direction due to deformation adjacent to and within younger dextral faults zones. This pattern is most obvious near the Clark, Hell Hole Canyon, and San Felipe fault zones (Steely, 2006; Belgarde, 2007). The antiformal West Salton

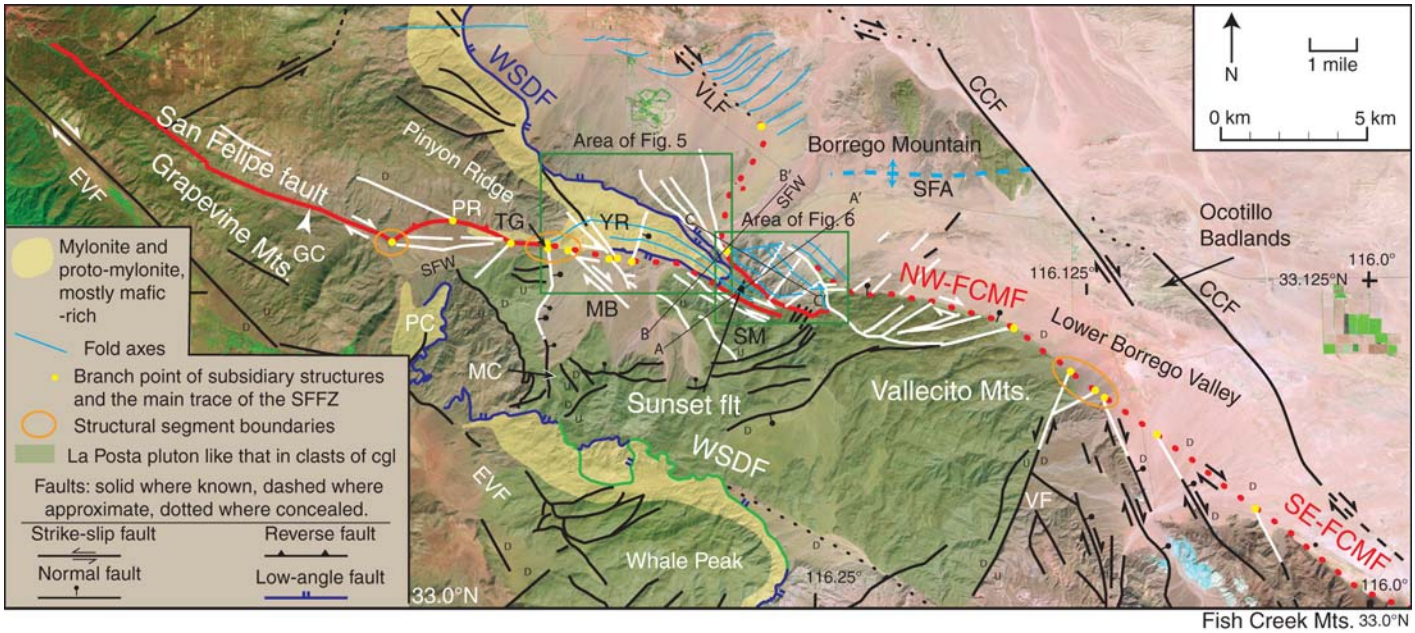

Figure 3. The central portion of the San Felipe fault zone near Yaqui Ridge in red and white. Red denotes the major traces, and white denotes smaller splays and connector faults. Note the overall contractional left bend in the fault zone from the SE Fish Creek Mountain fault to the San Felipe fault. Faults of the West Salton detachment fault (WSDF) are blue. Active parts of the WSDF are green. Mescal Bajada structural segment is east of Tamarisk Grove (TG) and Pinyon Ridge structural segment is west of it. CCF—Coyote Creek fault; EVF—Earthquake Valley fault; GC—Grapevine Canyon; MB—Mescal Bajada; PC—Plum Canyon; NW-FCMF—Northwest Fish Creek Mountain fault; PC—Plum Canyon; SE-FCMF—Southeast Fish Creek Mountain fault; SFA—San Felipe Anticline; SFW—San Felipe Wash; SM—Sunset Mountain; TG—Tamarisk Grove; VF—Vallecito fault; VLF—Veggie Line fault; WSDF—West Salton detachment fault; YR—Yaqui Ridge. Uncolored basement west of the WSDF consists of biotite schist, fine-grained tonalite, and mafic-rich tonalite unlike clasts in the Sunset Conglomerate. Structures were compiled from Dibblee (1984); Kairouz (2005); Steely (2006); and this study.

detachment fault at Whale Peak may be the only documented original corrugation to display a reversal in dip directions. Preliminary paleomagnetic data there are consistent with ~30° of postdetachment tightening of the originally more open antiformal corrugation (B. Housen and G. Axen, 2006, written commun.). The structural geometries of the West Salton detachment fault are complex, mostly beyond the scope of this paper, and the subject of ongoing research.

Stratigraphy

Overview

Sedimentary rocks in the San Felipe–Borrego subbasin of the Salton Trough have an aggregate thickness of roughly 5 km and include the Late Miocene (?) to Pliocene Imperial Group, the Pliocene to Pleistocene Palm Spring Group, and the Pleistocene Ocotillo and Brawley Formations (Fig. 4) (Dibblee, 1954, 1984, 1996; Morley, 1963; Reitz, 1977; Lutz, 2005; Kirby, 2005; Dorsey, 2006; Steely, 2006; Belgarde, 2007). Sediments of the Imperial and Palm Spring groups accumulated in a large supradetachment basin during generally E- to ESE-directed slip across the West Salton detachment fault (Kairouz, 2005; Steely, 2006). These deposits record complex interactions among different geologic structures, the Colorado River delta system, fluvial systems flowing off the Peninsular Ranges, and the Gulf of California seaway (Winker and Kidwell, 1986, 1996, 2002; Axen and Fletcher, 1998; King et al., 2002; Dorsey, 2006; Steely, 2006; Dorsey et al., 2007).

Postdetachment deposits of the early to middle Pleistocene Ocotillo Formation and its finer grained lateral equivalent, the Brawley Formation, overlie the older basin-fill deposits along a contact that changes laterally from conformable to an angular unconformity (Figs. 2 and 4) (Dibblee, 1984; Lutz, et al., 2006; Kirby et al., 2007). Below we provide a brief summary of the Pliocene Palm Spring Group, and then focus on postdetachment Pleistocene deposits that accumulated at the SW margin of the San Felipe–Borrego subbasin (Fig. 2).

Syndetachment Stratigraphy

Palm Spring Group

Diablo Formation, Olla Formation, and Canebrake Conglomerate. The Plio-Pleistocene Palm Spring Group conformably overlies the Imperial Group and includes the laterally equivalent Diablo and Olla Formations and Canebrake Conglomerate, and the overlying Borrego and Hueso Formations (Fig. 4) (Dibblee, 1984, 1996; Winker and Kidwell, 1996). The Diablo Formation accumulated in the subaerial fluvial-deltaic part of the Colorado River system in the Salton Trough. Its sandstone is typically tan to yellow-orange and contains distinctive, rounded hematite-coated quartz grains derived from the Colorado Plateau (Winker, 1987; Winker and Kidwell, 1996; Steely, 2006; Dorsey et al., 2007). The Olla Formation is also fluvial but it contains >20%–50% locally derived sand derived from the Peninsular Ranges plutons (Winker, 1987; Winker and Kidwell, 1996; Kairouz, 2005; Kirby, 2005; Steely, 2006; Belgarde, 2007). The Diablo and Olla Formations pass laterally W and SW into locally derived Canebrake Conglomerate near Yaqui Ridge (Fig. 5). There the Canebrake Conglomerate is faulted against Cretaceous mylonitic rocks along the West Salton detachment fault.

Borrego Formation. The lacustrine Borrego Formation overlies the Diablo Formation along a complexly interbedded and gradational contact in the San Felipe–Borrego subbasin

(Fig. 4) (Dibblee, 1954, 1984; Dorsey et al., 2005; Kirby, 2005; Belgarde, 2007). The Borrego Formation may be up to ~1.6–1.8 km thick in the San Felipe Hills and Borrego Badlands and consists of claystone, mudstone, and lesser sandstone and marlstone (Tarbet and Holman, 1944; Bartholomew, 1968; Dibblee, 1984; Kirby, 2005). The Borrego Formation accumulated in a perennial freshwater to brackish lake that experienced few lake-level lowstands in the San Felipe Hills (Kirby et al., 2007). The sill of the Borrego lake depocenter is traditionally interpreted as the delta of the Colorado River (Dibblee, 1954), but may have been a now-buried structural barrier that blocked incursion of marine waters from the Gulf of California early during its deposition (Dorsey et al., 2005). Coarse pebbly sandstone is typically rare in the Borrego Formation but becomes common (up to ~50%) in the southwestern Borrego Badlands. There, we have found rare but distinctive clasts of well-cemented sandstone reworked from the underlying Diablo, Olla, or lower Borrego Formations in one conglomerate bed ~95 m below the top of the Borrego Formation.

Hueso Formation. In the Fish Creek–Vallecito basin, south of our study area (Fig. 2), the Borrego Formation is absent and the sandy to pebbly Hueso Formation is the chronostratigraphic equivalent (Winker, 1987; Winker and Kidwell, 1996; Dorsey, 2006). The Hueso Formation is ~0.9–1.3 km thick, 2.8–0.9 Ma, overlies the Diablo and Olla Formations, and is laterally equivalent to the upper part of the Canebrake Conglomerate (Johnson et al., 1983; Winker, 1987; Winker and Kidwell, 1996; Kairouz, 2005; Dorsey et al., 2006). It is coarser than the Borrego Formation, is locally derived, and contains no sediment from the Colorado River. Near Whale Peak, Canebrake Conglomerate that is laterally continuous with the upper part of the Hueso Formation is cut by the West Salton detachment fault (Kairouz, 2005). This relationship provides direct evidence that this part of the detachment fault continued to slip into the latest Pliocene and early Pleistocene.

The character and significance of the transition from the muddy Borrego Formation in the north to the sandy Hueso Formation in the south is poorly understood because the uplifted Vallecito and Fish Creek mountains now separate exposures of these two dissimilar but once-contiguous units (e.g., Dorsey et al., 2005; Kirby et al., 2007). Our study area east of Yaqui Ridge is one of the few locations that preserves sedimentary rocks in the area between exposures of the Hueso and Borrego Formations, and therefore should expose rocks of this age. However, the Borrego and Hueso Formations are absent along an angular unconformity between the Diablo

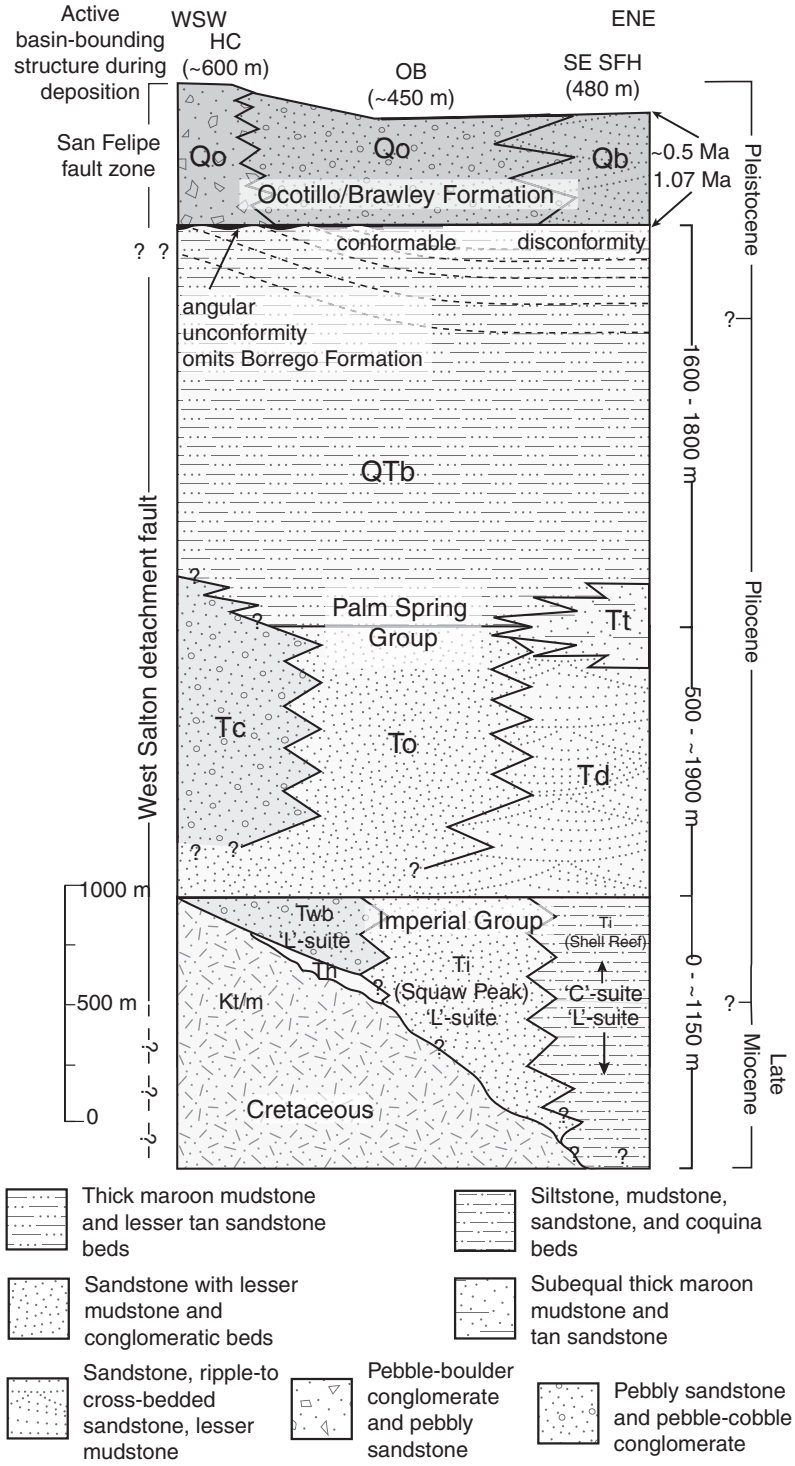

Figure 4. Generalized stratigraphic column for the SW Salton Trough showing laterally equivalent units, approximate thickness patterns, and active structures. Thicknesses of the Ocotillo and/or Brawley Formation are from this study at Harper Canyon (HC), and Kirby et al. (2007) at Ocotillo Badlands (OB) and SE San Felipe Hills (SE SFH). Other thicknesses are shown as the average of reported thicknesses (Morley, 1963; Reitz, 1977; Dibblee, 1984; Dorsey et al., 2006; Kirby, 2005; Lutz, 2005). Tc—Canebrake Conglomerate; To—Olla Formation; Td—Diablo Formation; Tt—Palm Spring–Borrego transitional unit; Ti—Imperial Formation; Th—Hawk Canyon Formation; Twb—West Butte Conglomerate; Kt/m—Cretaceous plutonic rocks and local metaplutonic and metasedimentary rocks; QTb—Borrego Formation; Qo—Ocotillo Formation; Qb—Brawley Formation.

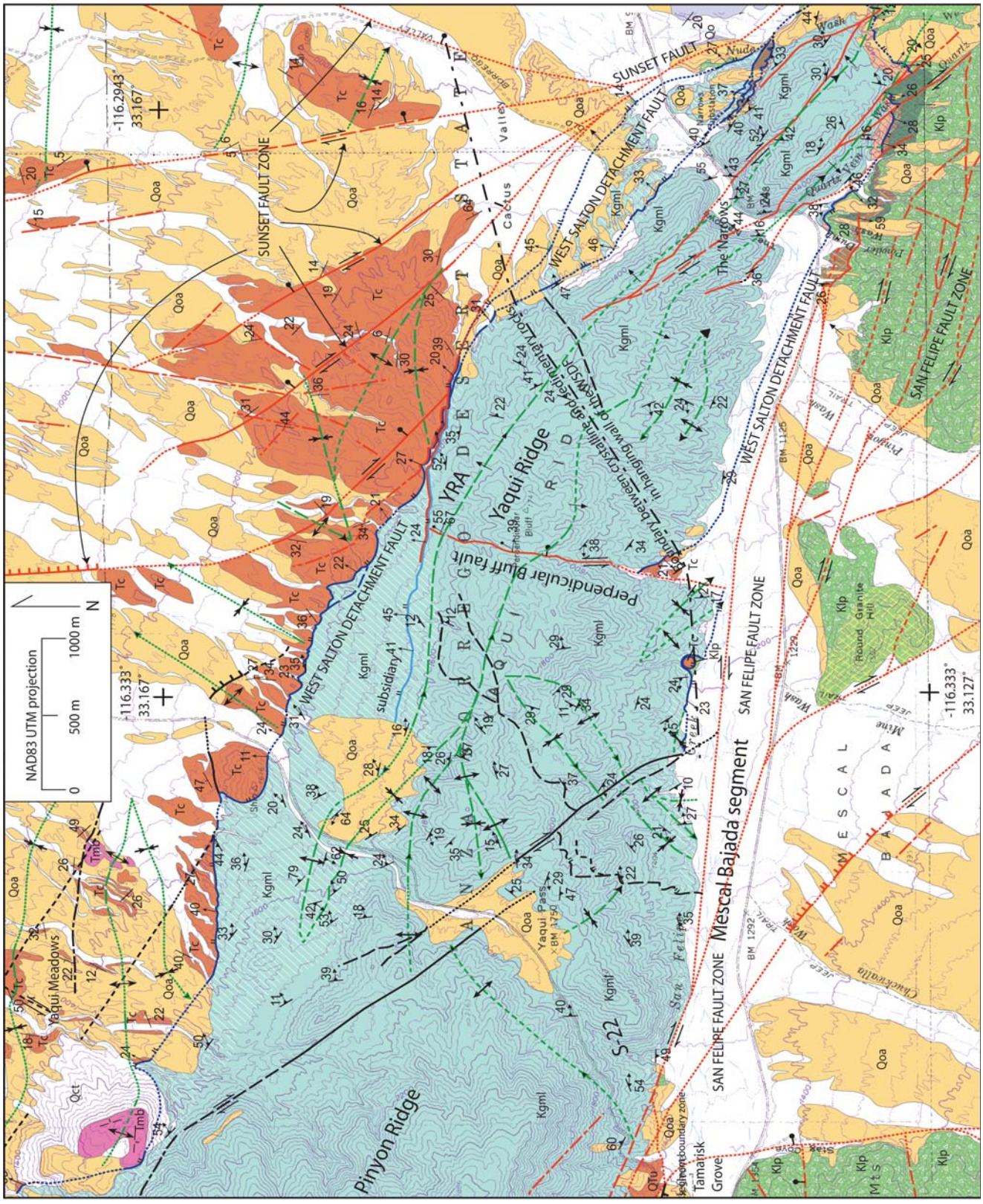

Figure 5. Simplified geological map of the Yaqui Ridge area. Modified from Steely (2006). Key and color scheme is the same as Figure 6. YRA—Yaqui Ridge antiform. Representative strike and dip data are shown for clarity. Additional data constrain positions of structures and interpretations in Figure 13. Faults are coded by color: West Salton detachment fault—blue, Faults of the San Felipe fault zone—red, other strike slip faults—black. UTM—Universal Transverse Mercator.

Formation and younger Sunset Conglomerate of the Ocotillo Formation. The absence of Borrego-age deposits in this area is due to erosion and/or nondeposition, as discussed below.

Postdetachment Stratigraphy

Ocotillo and Brawley Formations

The Ocotillo Formation is a widespread unit of coarse-grained alluvial sandstone, conglomerate, and interbedded finer grained lithologies (Fig. 4) (Dibblee, 1954; Bartholomew, 1968; Dibblee, 1984; Lutz et al., 2006; Kirby et al., 2007). The Brawley Formation is the finer grained, fluvial-deltaic lateral equivalent of the Ocotillo Formation (Kirby et al., 2007). The age of the Ocotillo and Brawley Formations is ca. 1.1–0.5 Ma based on magnetostratigraphy in the Borrego Badlands (Lutz, 2005; Lutz et al., 2006), Ocotillo Badlands (Brown et al., 1991), and San Felipe Hills (Kirby, 2005; Kirby et al., 2007). In the Borrego Badlands, the base of the Ocotillo Formation is ca. 1.05 Ma and the top is ca. 0.6 Ma (Lutz et al., 2006). In the San Felipe Hills, 18 km SE of the Borrego Badlands, the disconformable base of the laterally equivalent Brawley Formation is also ca. 1.1 Ma, and the erosional top of the formation is 0.5–0.6 Ma (Kirby et al., 2007).

The nearly synchronous progradation of pebble- to sand-dominated alluvial to fluvial deposits of the Ocotillo and Brawley Formations over the clay-rich lacustrine Borrego Formation has been interpreted to record major basin reorganization during initiation of the San Felipe and San Jacinto dextral strike-slip fault zones (Kirby et al., 2007; Lutz et al., 2006). The widespread and abrupt end of deposition of the Ocotillo and Brawley Formations at ca. 0.5–0.6 Ma in the San Felipe–Borrego subbasin probably reflects a second, less significant structural reorganization related to changes in the geometry and kinematics of the San Jacinto and San Felipe fault zones (Kirby, 2005; Lutz et al., 2006).

In this paper, we examine and describe a belt of conglomerate exposed along the northern flank of the Vallecito Mountains that was previously correlated to the Pliocene Canebrake Conglomerate (Dibblee, 1984; Winker and Kidwell, 1996). We show that it is instead a proximal facies of the Pleistocene Ocotillo Formation. Because this belt is not contiguous with other outcrops of the Ocotillo Formation, we informally name this unit the Sunset Conglomerate of the Ocotillo Formation. We then use this coarse basin-margin facies to locate and infer the age of the active basin-bounding fault system and to further refine and test the hypotheses of Lutz et al. (2006) and Kirby et al. (2007) regarding the age and evolution of the San Felipe fault zone.

Sunset Conglomerate

Description. The Sunset Conglomerate is exposed NE of the Sunset fault (a short strand of the San Felipe fault zone) and SW of the Fish Creek Mountains fault. The unit covers an area ~5.7 km long and up to 2.6 km wide (Fig. 6). The NW-striking dextral-oblique Sunset fault places Sunset Conglomerate and locally exposed underlying Pliocene Palm Spring Group against Cretaceous tonalite SW of the fault. The Sunset Conglomerate lies along a slight angular (10°–15°) unconformity on the Canebrake, Olla, and Diablo Formations of the Palm Spring Group, and the intervening Borrego Formation is absent across this contact (Fig. 6). The Sunset Conglomerate is at least 600 m thick based on geological cross sections and map-based estimates (Figs. 6 and 7). Lateral equivalents of the Sunset Conglomerate are inferred to exist in the subsurface E and ENE of the Fish Creek Mountains fault.

The Sunset Conglomerate consists of light-gray to gray-tan, moderately to weakly cemented, poorly sorted coarse to pebbly sandstone, pebble to cobble conglomerate, and angular to subrounded cobble to boulder conglomerate. Overall this unit coarsens upsection from pebbly sandstone near the base to boulder conglomerate with angular to rounded clasts near the top. It also coarsens laterally from coarse sandstone ~2 km NE of the fault to angular cobble to boulder conglomerate near the fault in the SW. Bedding in proximal deposits near the Sunset fault is typically characterized by 0.5- to 2-m-thick interbedded coarser and finer conglomerate beds that locally contain outsized clasts of small to large boulders up to 4 m in diameter (Fig. 8). Proximal deposits contain <20%–30% sand and distal deposits typically contain >50% sand. Distal exposures of the Sunset Conglomerate are characterized by weakly to moderately bedded, poorly sorted, planar to low-angle, trough cross-stratified, coarse to pebbly sandstone and lesser pebble to cobble conglomerate (Fig. 8). Beds average 1–50 cm thick and tonalite clasts range from angular to subrounded. Overall, distal exposures are tanner in color than exposures proximal to the Sunset fault and, although not extensively studied, contain a significant population of pink hematite-coated rounded quartz sand grains.

Imbricated clasts (n = 58 sites, 3–10 clasts per site) and trough axes (n = 3 sites, 3–5 axes per site) show overall paleotransport toward N57°E ± 12° when corrected for bedding tilt, with a spread of 120° about the average direction (Fig. 9). This ENE-directed paleoflow is approximately perpendicular to the N25°W–N55°W strike of the Sunset fault (Figs. 6 and 9).

Biotite-bearing tonalite (La Posta–type, see key of Fig. 6) and associated plutonic rocks (85%) dominate clasts in the Sunset Conglomerate, with lesser metamorphic rocks (8%) and deformed and chloritically altered plutonic rocks (3%) (Figs. 8A–E and 10). A small but significant population of clasts (average = 4%) are composed of distinctive light tan to tan-pink sandstone (Figs. 8 and 10). These sandstone clasts contain pink rounded and hematite-coated quartz grains derived from the Colorado River, are locally present throughout the Sunset Conglomerate, and account for up to 10% of clasts at some locations.

Depositional processes and environment. We interpret the poorly sorted, matrix-supported, pebble to angular boulder conglomerate with outsized clasts near the Sunset fault as debris-flow deposits that accumulated on a steep arid alluvial fan. Northeastward lateral fining into poorly sorted sandstone and sandy pebble conglomerate reflect a down-fan transition into sandy and gravelly sheet-flood deposits with minor shallow stream channels. The lateral continuity of these facies and the paleoflow indicators suggest deposition in the upper and middle part of an alluvial fan that was bounded on its SW margin by the Sunset fault.

Provenance and recycling. Biotite-bearing La Posta–type tonalite clasts, which dominate the Sunset Conglomerate (64%), are identical to plutonic rocks on the SW side of the Sunset fault (Figs. 5, 6, and 10). La Posta–type plutonic rocks are widely exposed south of a poorly understood, approximately west-trending boundary with Canebrake Conglomerate in the hanging wall of the West Salton detachment fault at Yaqui Ridge (Fig. 5). More mafic Granite Mountain–type tonalite and mylonitic rocks, which are widespread in the immediate footwall of the West Salton detachment fault, are exposed along Yaqui Ridge less than 500 m west of the westernmost exposure of the Sunset Conglomerate on the N-NW side of this boundary, and are not present as clasts in the Sunset Conglomerate (Figs. 3, 5, 6, and 10).

Distinctive well-cemented, tan-pink sandstone clasts, like those in the Sunset Conglomerate, are present in the Ocotillo Formation throughout the western Salton Trough (Fig. 8). This clast type was also found in one conglomerate bed in the upper Borrego Formation of the southwestern Borrego Badlands. Hematite-coated, well-rounded quartz grains are diagnostic of sand derived from the Colorado River (Merriam and Bandy, 1965) and are especially abundant in fluvial-deltaic sandstone of the Diablo Formation of the Palm Spring Group, a unit that contains many large well-cemented concretions (Winker, 1987; Winker and Kidwell, 1996). The upper Imperial Group and Borrego Formation contain less of this distinctive sandstone, have few

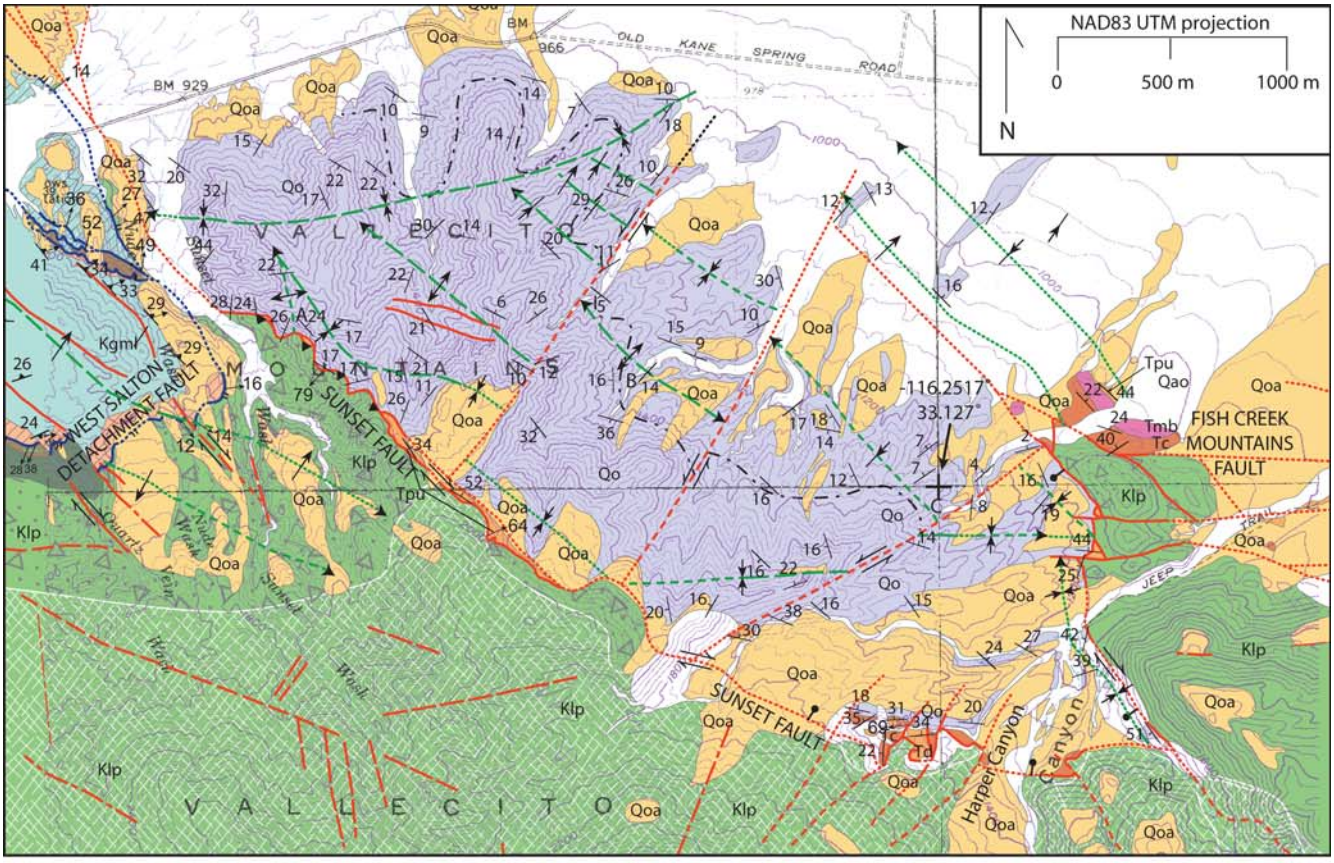

Q Quaternary deposits: includes Recent and older alluvium, colluvium, and talus

Qoa Quaternary old alluvium deposits

Qo Quaternary Ocotillo Formation (Sunset conglomerate)

QTu undivided Quaternary-late Tertiary deposits in San Felipe Wash

Palm Spring Group

Tpu Pliocene Olla and Diablo Formations

Tmb Pliocene megabreccia deposit

Tc Pliocene Canebrake Conglomerate

Klp Cretaceous 'La Posta-type' tonalite

Kgml Cretaceous mixed 'Granite Mountain-' and 'La Posta-type' diorite and tonalite (contains much mylonite and proto-mylonite)

cg cohesive fault gouge/microbreccia

Ksm Cretaceous biotite/psammitic schist and other metasedimentary rocks

cx brittle and lesser ductile chloritic fault rocks

WSDF alteration/damage zone

heavily to moderately fractured rock

brecciated rock

Approximate boundary between coarse- (above) and fine-grained (below) Ocotillo Formation

18 Strike and dip of bedding

29 Solid-state mylonitic foliation with lineation direction (Eastern Peninsular Ranges Mylonite Zone)

16 Fault dip and dip direction

Faults: solid where known, long dash where approximate, short dash where inferred, dotted where concealed.

Normal fault: ball and bar on down-thrown side

Strike-slip fault: arrows indicate sense of separation

Thrust fault: barb on up-thrown side

Low-angle fault: ticks on hanging wall

Fault scarp: ticks on down-thrown side

Lineament from aerial photographs

Fold axes: solid where known, long dash where approximate, short dash where inferred, dotted where concealed.

plunging anticline

plunging syncline

plunging monocline

Figure 6. Simplified geologic map of the folded Sunset Conglomerate and bounding structures. Figure 5 slightly overlaps the western edge of this map. Faults of the San Felipe fault zone (SFFZ) are red and faults of the West Salton detachment fault (WSDF) are blue. Modified from Steely (2006). Note the changing dip-direction along the strike of the Sunset fault, consistent with its being mostly a strike-slip fault.

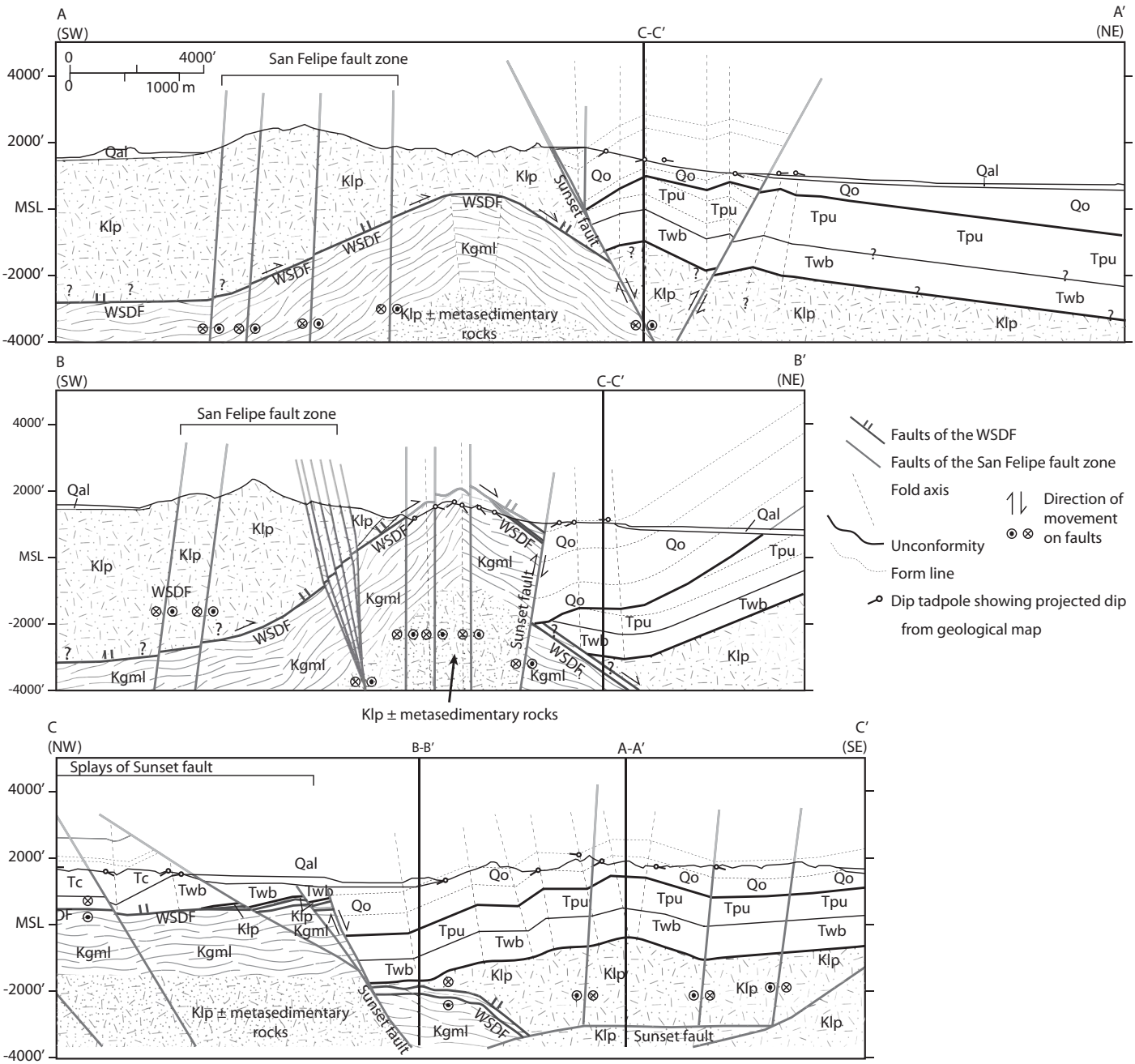

Figure 7. Geological cross section across Yaqui Ridge and one section constructed parallel to Yaqui Ridge. See Figure 3 for the locations of cross-section lines. Kgml—Cretaceous Granite Mountain–type diorite and granodiorite; Klp—Cretaceous La Posta–type tonalite; Qal—Quaternary alluvium; Qo—Quaternary Ocotillo Formation (Sunset Conglomerate); QTu—undifferentiated Quaternary-Tertiary deposits; Tc—Pliocene Canebrake Formation; Td—Pliocene Diablo Formation; Tmb—Pliocene Yaqui Ridge megabreccia; To—Pliocene Olla Formation; Tpu—Pliocene Palm Spring Group undifferentiated; Twb—Pliocene West Butte Conglomerate; WSDF—West Salton detachment fault.

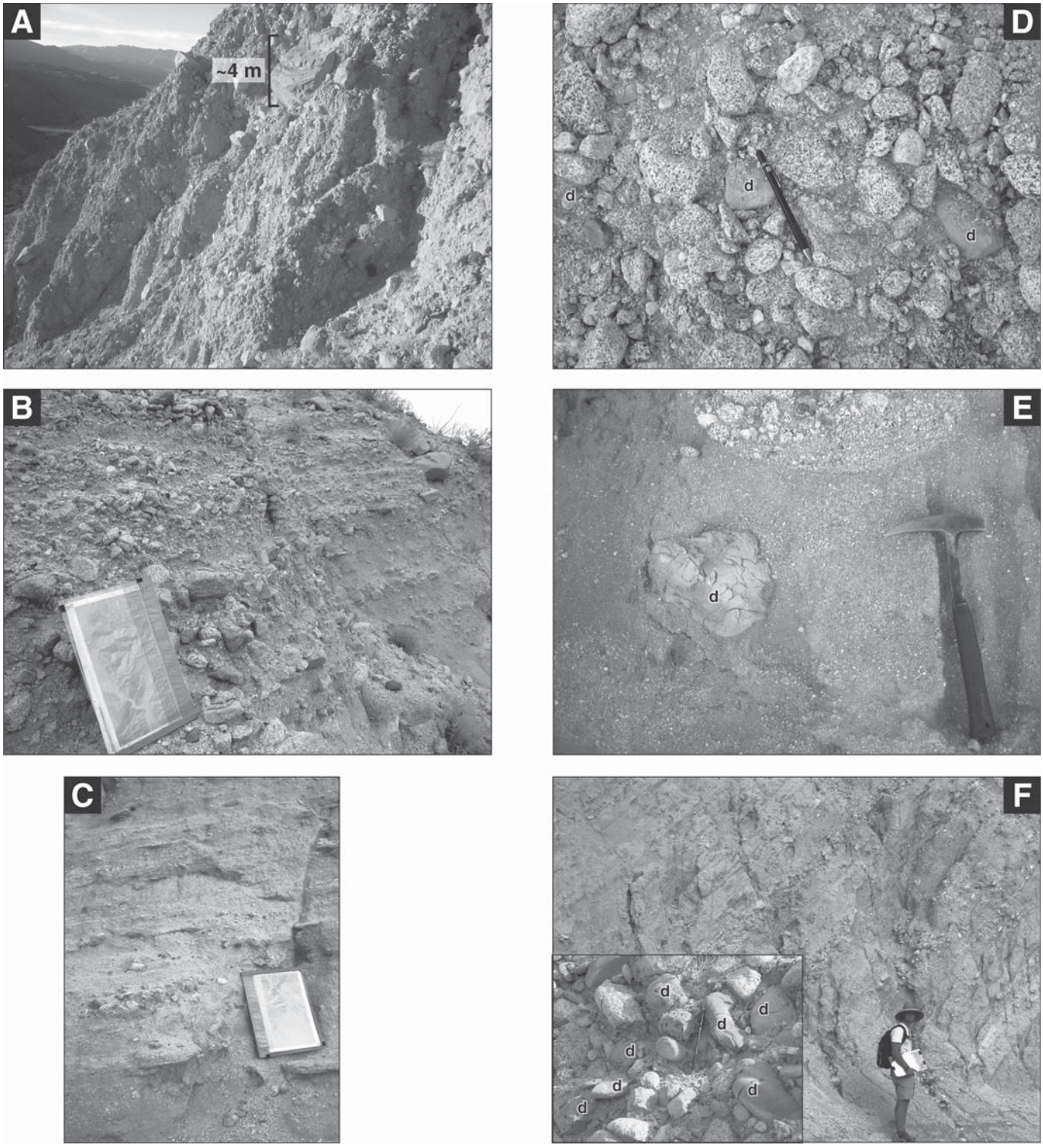

Figure 8. Photographs of the Sunset Conglomerate. (A) Sunset Conglomerate <30 m from the Sunset fault, large boulder is ~4 m in diameter. (B) Sunset Conglomerate ~1 km NE of Sunset fault, map board is 28 × 44 cm. (C) Sunset Conglomerate ~2 km NE of the Sunset fault. (D) Sunset Conglomerate dominated by La Posta–type tonalite with several prominent tan recycled sandstone clasts derived from the Diablo Formation (d). (E) Base of conglomerate-filled channel and outsized cobble of Diablo Formation in the Sunset Conglomerate. (F) Tilted pebbly sandstone beds of the Ocotillo Formation in the Ocotillo Badlands. Inset of Ocotillo Formation dominated by recycled clasts derived from the Diablo Formation (d).

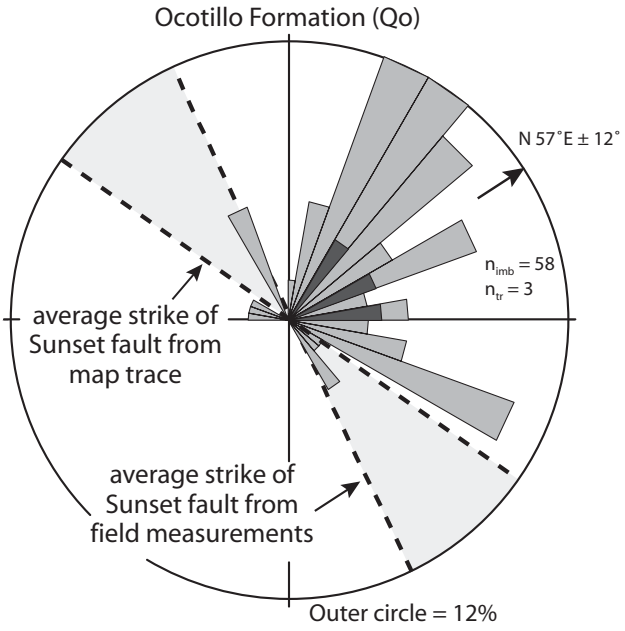

Figure 9. Rose diagram of paleocurrents from the Ocotillo Formation (Sunset Conglomerate). Light-gray petals are measurements from tilt-corrected poles to clast imbrications; dark-gray petals are measurements from tilt-corrected trough axes. Bidirectional trough axes are plotted in the same quadrant as the unidirectional imbrications. Nimb—number of imbrications; ntr— number of trough axes.

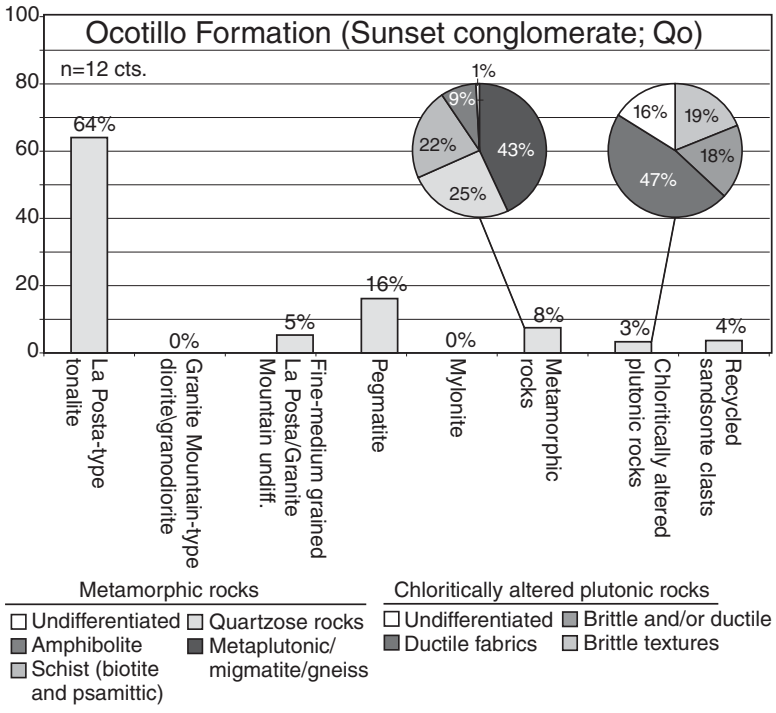

Figure 10. Clast count for the Ocotillo Formation (Sunset Conglomerate). Pie charts represent the percentage of different chloritic or metamorphic rocks within the binned populations. Each clast count represents 50 clasts at a single location. Clast populations are labeled with percentages (18%).

concretions, weather to other colors, and/or have weak cementation (Reitz, 1977; Dibblee, 1984; Kirby, 2005). No shells from the Imperial Group or mudstone clasts from the Borrego Formation were observed in the Sunset Conglomerate.

The presence of distinctive sandstone clasts in the Sunset Conglomerate records recycling of older Pliocene basin-fill sedimentary rocks from the source area of the younger Sunset Conglomerate. We interpret the hematite-coated quartz grains in sandy matrix of the distal Sunset Conglomerate to be Colorado River–derived sand grains recycled from the same older basin fill. For the reasons listed above, the Diablo Formation is the most likely source of the tan recycled sandstone clasts and sand grains.

Metamorphic and chloritically altered clasts comprise ~10% of the clasts in the Sunset Conglomerate (Fig. 10). These lithologies cannot be derived from the large body of La Posta–type plutonic rocks SW of the Sunset fault and also do not match mylonites from the immediate footwall of the West Salton detachment fault near the Sunset Conglomerate. The damage zone in the hanging wall of the West Salton detachment fault and the Pliocene Canebrake Conglomerate contain these rock types (~34% of the clasts in the Canebrake Conglomerate have this composition; Steely, 2006). The Canebrake Conglomerate underlies the Sunset Conglomerate and occurs in the hanging wall of the West Salton detachment fault near the Sunset Conglomerate. The proximity of the underlying Canebrake Conglomerate and the erosion implied by the angular unconformity between the Sunset Conglomerate and the Canebrake Conglomerate suggest that the small population of metamorphic and chloritically altered clasts (~10%) is most likely reworked from the older Canebrake Conglomerate nearby. More distant source areas may also have contributed.

Correlation and age. Based on the similar stratigraphic position, thickness, basal contact, grain size, depositional environments, paleoflow, composition, and sandstone clasts recycled from the Palm Spring Group, we interpret the Sunset Conglomerate to be a proximal facies of the Ocotillo Formation (Fig. 4). Because the Sunset Conglomerate overlies the Palm Spring Group along an angular unconformity, it must be younger than the Palm Spring Group and thus cannot correlate to the Canebrake Conglomerate or West Butte conglomerate (Fig. 4). The Ocotillo Formation and much older West Butte conglomerate are the only units in the San Felipe–Borrego basin that have angular unconformities at their base like the Sunset Conglomerate (Dibblee, 1984; Brown et al., 1991; Lutz et al., 2006; Steely, 2006; Kirby et al., 2007). The ~600 m thickness of the Sunset Conglomerate is

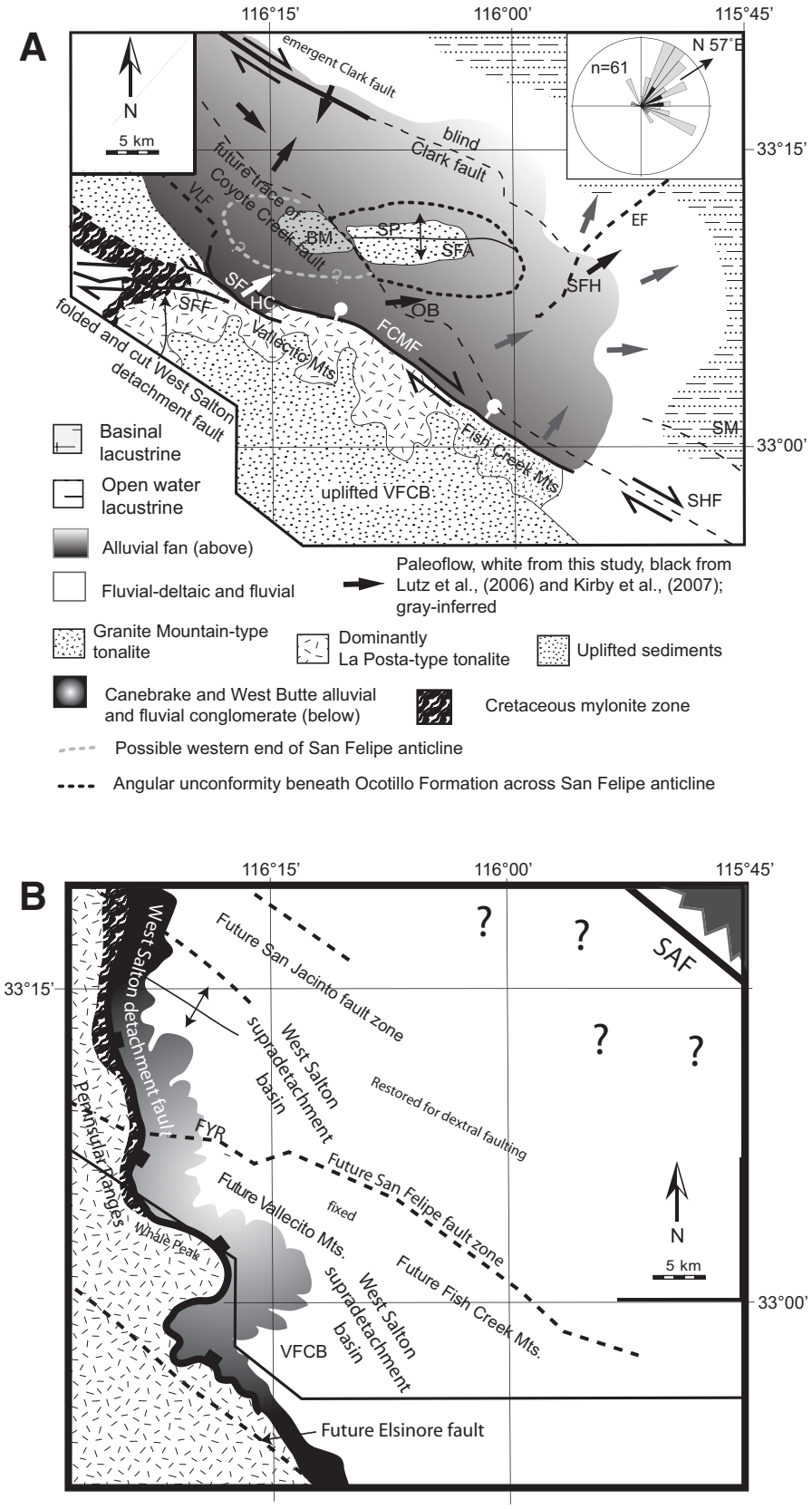

Figure 11. (A) Paleogeography during deposition of the Ocotillo and Brawley Formations just after 1 Ma. BM—Borrego Mountain; EF—Extra fault; FCMF—Fish Creek Mountains fault; VFCB—Fish Creek–Vallecito basin; HC—Harper Canyon; SFA—San Felipe anticline; OB—Ocotillo Badlands; SFH—San Felipe Hills; SFF—San Felipe fault; SF—Sunset fault; SHF—Superstition Hills fault; SM—Superstition Mountains; SRM—Southern Santa Rosa Mountains; VLF—Veggie line fault. Rose diagram shows paleoflow from the Sunset Conglomerate unit of the Ocotillo Formation near Harper Canyon. Lighter shades represent finer grain size. Modified from Kirby et al. (2007). (B) Paleogeography ca. 3–4 Ma during simultaneous slip across the West Salton detachment fault and the San Andreas fault (SAF). Younger dextral offsets were restored NE of the San Felipe fault zone. Note outline of area that matches Figure A.

similar to, but somewhat thicker than the maximum thickness of the Ocotillo Formation in the Borrego Badlands (~500 m; Lutz et al., 2006), Ocotillo Badlands (450 m), and the correlative Brawley Formation in the eastern San Felipe Hills (480 m) (Kirby et al., 2007). This is consistent with our correlation.

Regionally, the Ocotillo Formation is dominated by sandy conglomerate and sandstone, and records sheet-flood deposition in medial to distal alluvial fan, bajada, and fluvial environments (Lutz et al., 2006). The laterally equivalent Brawley Formation records deposition in distal fluvial, fluvial-deltaic, and lacustrine environments (Kirby et al., 2007). The Sunset Conglomerate was deposited in proximal to medial alluvial fan environments upslope of these medial to distal fan deposits. Its thickness and grain size patterns show that it is syntectonic to slip on the dextral-oblique Sunset fault. The Ocotillo and Brawley Formations are also interpreted as syntectonic deposits related to initiation and slip on the dextral San Felipe fault zone SW of the San Felipe–Borrego subbasin (Lutz et al., 2006; Kirby et al., 2007). Our study strongly supports their interpretation.

Paleocurrents in the Ocotillo Formation are spatially variable in the SW Salton Trough and are generally directed E to ENE in the central and eastern part of the subbasin (Fig. 11; Lutz et al., 2006; Kirby et al., 2007). The Ocotillo Formation in the Borrego Badlands thickens northeastward toward the Clark fault of the San Jacinto fault zone (Lutz et al., 2006), and Kirby et al. (2007) document southwestward

coarsening toward the San Felipe fault zone. The thinnest sections are in the middle of the basin across the crest of the San Felipe anticline (Lutz et al., 2006; Kirby et al., 2007). The Sunset Conglomerate also has NE-directed paleotransport and coarsens SW toward the dextral-oblique Sunset strand of the San Felipe fault zone. The somewhat greater thickness of the Sunset Conglomerate compared to that of the Ocotillo and Brawley Formations in the San Felipe Hills and Ocotillo Badlands is consistent with overall SW thickening toward the main basin-bounding faults of the San Felipe–Borrego basin (Fig. 11). Clast lithologies in the Ocotillo Formation and Sunset Conglomerate are nearly identical. Both units contain plutonic and metamorphic rocks derived from local highlands, and sandstone clasts and sand grains recycled from older basin fill of the Palm Spring Group (Figs. 8 and 11) (Bartholomew, 1968; Dibblee, 1984; Lutz et al., 2006; Kirby et al., 2007).

These data indicate that the Sunset Conglomerate is the proximal lateral equivalent of the Ocotillo and Brawley Formations, which are well dated elsewhere at ca. 1.1–0.6 Ma (Figs. 4 and 11; Lutz et al., 2006; Kirby et al., 2007). Thus the age of the Sunset Conglomerate is also inferred to be ca. 1.1–0.6 Ma, although the angular unconformity and absence of Borrego Formation beneath the Sunset Conglomerate introduce some uncertainty into this age assignment. Because the entire Ocotillo Formation accumulated in only ~0.5 m.y., the basal Sunset Conglomerate is probably no more than ~0.2 Ma m.y. younger or older than other parts of the Ocotillo Formation. We therefore estimate the age of the basal Sunset Conglomerate to be ca. 1.1 ± 0.2 Ma, which means that the oldest synkinematic deposits are likely to be slightly younger or older than basal deposits of the Pleistocene Ocotillo Formation, where it has been precisely dated.

STRUCTURAL GEOLOGY

In this section we examine the geometry and kinematics of the San Felipe fault zone to establish the structural setting of the postdetachment deposits, to characterize segments and structural features along the San Felipe fault zone, and to assess the relationship between the San Felipe fault zone and the West Salton detachment fault.

San Felipe Fault Zone

Overview

The San Felipe fault zone is a major structure that is almost as long as the better known faults of the San Jacinto and Elsinore fault zones. About 150 km long, it is a dextral to dextral-oblique fault that strikes NW to WNW and consists of anastomosing and branching fault strands (Figs. 2 and 3). Strands of the fault zone were first described by Dibblee (1954, 1984) and Rogers (1965) in the SW Salton Trough as a set of strike-slip faults that bound the south side of Yaqui Ridge and the N side of the Vallecito and Fish Creek Mountains, connecting west-northwestward to the Agua Caliente, Aguanga, and Murrieta Hot Springs faults (Kennedy and Morton, 2003). Based on prior nomenclature and studies (e.g., Dibblee, 1984, 1996), we use the name San Felipe fault zone to refer to the entire collection of fault strands from Murrieta Hot Springs in the NW to the front of the Fish Creek Mountains in the SE. We restrict the name San Felipe fault to the portion of the fault zone that is south of Yaqui and Pinyon ridges and extends NW into Grapevine Canyon (Rogers, 1965; Wagner, 1996). We introduce a new name, the Fish Creek Mountains fault, for the eastern continuation of the San Felipe fault zone on the NE margin of the Vallecito and Fish Creek mountains (e.g., Dibblee, 1954, 1984, 1996; Kirby, 2005). Dibblee (1954, 1984, 1996) incorrectly mapped the Fish Creek Mountains fault as continuous with the San Felipe fault. In this study we identify and analyze three structural segments along the central ~15 km of the San Felipe fault zone—the Pinyon Ridge, Mescal Bajada, and Northwest Fish Creek Mountain segments (Fig. 3)—and describe the newly identified Sunset fault between the latter two segments.

The central San Felipe fault zone has an overall sigmoidal map pattern, with N55°W–striking faults along Grapevine Canyon and the NE side of the Fish Creek and Vallecito Mountains (Fig. 3). These segments are connected by a ~15-km-long zone of transpressive E-W–striking faults and folds south of Pinyon and Yaqui ridges. This part of the fault zone consists of the Pinyon Ridge and Mescal Bajada structural segments (Fig. 3). Boundaries of the segments coincide with the tips of major folds, bends in the fault, left and right steps, branch points in the fault zone, and major changes in structural style within the fault zone (Fig. 3; Steely, 2006). The Pinyon Ridge and Mescal Bajada structural segments are only 6.75 and 9 km long, respectively, and despite their distinct characteristics might instead be subsegments of a single, longer segment (Fig. 3).

North of the Mescal Bajada segment, the West Salton detachment fault dips ~20° SW in its westernmost exposure on the south side of Yaqui Ridge (Fig. 5). The detachment fault is also exposed south of the San Felipe fault near Plum Canyon 5.8 ± 2.8 km farther west (Fig. 3), although the cutoff of the detachment fault is buried by alluvium along San Felipe Wash. Slickenlines measured on the main subvertical fault strand within the Pinyon-Mescal segment boundary are dominantly subhorizontal and suggest that horizontal displacements exceed vertical displacements along this part of the fault zone. The distributions of rock units on either side of the Mescal Bajada segment also indicate horizontal displacements in excess of vertical displacements (Steely, 2006). Taken together, these data suggest that the 5.8 ± 2.8 km right separation measured from the displaced detachment fault is mostly the result of dextral slip across the fault zone. Fault strands within the Pinyon Ridge and Mescal Bajada segments displace and fold late Pleistocene deposits.

The structural geology of the fault zone is complex along the Pinyon Ridge and Mescal Bajada segments, and there are several subsidiary faults and folds that diverge from the central fault zone. One moderately to steeply ENE-dipping fault that crosses Yaqui Ridge (Perpendicular Bluff fault) is 1.8 km long (Fig. 5), and has slickenlines that rake from 25° to 90°N (n = 3). A prominent E-facing topographic scarp along this fault suggests that there is a normal component of displacement. In the south this fault displaces the West Salton detachment fault in a sinistral-normal sense and produces ~500 m of left-separation. To the N the fault does not cross a 1- to 2-km-long subsidiary footwall strand of the West Salton detachment fault with moderate N dips (Fig. 5). The Perpendicular Bluff fault may be cut by the detachment strand, it may lose displacement northward, as indicated by northward thinning of the prominent alteration zone, or it may transfer some slip onto a part of the subsidiary detachment fault.

Three left-stepping, en echelon fault strands comprise a major structural boundary at the E end of the Mescal Bajada segment of the San Felipe fault zone (Fig. 3). From NW to SE these are the San Felipe fault, the Sunset fault, and the Fish Creek Mountains fault (Figs. 3, 5, and 6). These three faults bound two distinct contractional stepovers that we collectively name the Narrows stepover. The Sunset Conglomerate is folded in the stepover between the Sunset and Fish Creek Mountains faults. The older Eastern Peninsular Ranges mylonite zone and West Salton detachment fault either have an older foldlike geometry or are folded in the stepover between the San Felipe and Sunset fault. Both the mylonite and detachment fault are cut by subsidiary small-offset dextral faults between the Sunset and San Felipe faults (Figs. 5 and 6). The folded mylonite and detachment fault define the Yaqui Ridge antiform (Schultejann, 1984). The antiform has a limited lateral extent

and ends or bends southwestward at the saddle (and possible wind gap) that defines the boundary between Yaqui and Pinyon Ridges. The antiform does not appear to persist westward (Fig. 5).

Sunset Fault

The NW-striking Sunset fault is located between the San Felipe fault to the west and the Fish Creek Mountains fault to the east and parallels the San Felipe fault for ~7.5 km (Figs. 3, 5, and 6). The boundary between the Sunset fault and the Fish Creek Mountains fault is a faulted transpressional left stepover in which the two faults are parallel for ~2.5 km and bound complexly folded and faulted Pleistocene Sunset Conglomerate (Figs. 3 and 6). Along most of its length the Sunset fault places the Sunset Conglomerate and units of the underlying Palm Spring Group against plutonic Cretaceous tonalite (Fig. 6). Locally, thin belts of moderately to steeply dipping fault-bound slivers of Palm Spring Group are upturned along the fault.

The Sunset fault zone persists for ~10.8 km from near Harper Canyon WNW to the N side of Yaqui Ridge. It changes west-northwestward from a single fault to a 4-km-wide by 5-km-long horsetail splay of small faults that vary up to ~90° in strike (Figs. 3, 5, and 6). Immediately WNW of San Felipe Wash the main strand of the Sunset fault becomes an E- to ESE-dipping normal fault that is buried by the alluvium of San Felipe Wash. This normal fault has ~1 km of dip-slip separation based on stratigraphic and structural relationships and analyses of cross sections (Fig. 7C; Steely, 2006). Other subsidiary strands strike NNW to WNW, have small offsets, and cut and uplift older alluvium and Canebrake Conglomerate (Fig. 5). Degraded fault scarps are present along portions of the horsetail splay in older alluvium.

Plutonic rocks SW of the single-stranded part of the Sunset fault are brecciated in a 0.5- to 5-m-wide zone. They are locally bleached white and have a chalky texture (Fig. 6). Fracturing is well developed up to several hundred meters from the fault surface (Fig. 6). The tonalite in the hanging wall of the West Salton detachment fault is also brecciated for hundreds of meters above the detachment, and this damage zone has a folded form coincident with the Yaqui Ridge antiform. The damage zone SW of the Sunset fault overlaps with the older damage zone above the detachment fault.

Southeast of the horsetail splay, the Sunset fault strikes N55°W ± 10°, and three-point analyses shows that it is usually steep and changes both its dip and dip-direction along strike (Fig. 5). Near San Felipe Wash the fault dips steeply SW, near Harper Canyon the fault dips moderately to steeply ENE, and in between it is vertical (Figs. 6 and 7). Measurements from primary fault surfaces ($n = 12$) further document the waviness and variable dip direction of the fault (Fig. 12A).

The Sunset fault zone preserves complex slickenline patterns consistent with both strike-slip and dip-slip movements (Fig. 12A). These data and the map relationships suggest that the Sunset fault has complex slip patterns with dominant dextral strike-slip deformation and less NE-down slip. Although no shear-sense indicators were observed along the fault, its variable dip direction, overall NW strike, steep to moderate dip, and proximity to other similarly oriented faults with demonstrable dextral offset indicate that the Sunset fault is a dextral fault with smaller reverse and normal components of slip (Fig. 7).

The absence of displaced steeply dipping markers prevents a precise measurement of offset across the Sunset fault. A maximum slip estimate can be made from the provenance, grain size, and paleocurrents of the Sunset Conglomerate. Provenance studies show that ~64% of clasts in the conglomerate were derived from La Posta–type plutonic rocks (and 85% from all La Posta–related rock types) that are widespread in the hanging wall of the West Salton detachment fault. There are no clasts of mylonite or Granite Mountain–type tonalite derived from the footwall of the detachment, despite the footwall being in close proximity to the conglomerate. The tonalite clasts include angular boulders up to 4-m diameter near the Sunset fault (Fig. 8). This relationship requires that the Sunset Conglomerate was close to a La Posta–type tonalite source area during deposition. La Posta–type tonalitic rocks have a unique spatial distribution in this area and are only exposed E and S of Yaqui and Pinyon Ridges. This rock type is easy to identify because the mafic minerals are mostly biotite and are not abundant (green shading in Fig. 3) (Steely, 2006). Exposures of La Posta–type tonalite in the Whale Peak and Pinyon Ridge areas cannot be the source because they lie structurally beneath a thick carapace of mylonite and protomylonite border phases of the La Posta pluton (Granite Mountain type) that are notably more mafic in composition and are not present in clasts of the Sunset Conglomerate (Fig. 3; Kairouz, 2005; Steely, 2006). Based on the very coarse clast size of some proximal Sunset Conglomerate (Fig. 3) and fault-perpendicular paleocurrents, we infer that the Sunset Conglomerate must have been located directly NE of La Posta–type tonalite during deposition.

If we use the westernmost outcrop of La Posta–type tonalite above the West Salton detachment fault as our most distant sediment dispersal point, then slip on the Sunset fault is limited to less than 5 km of dextral separation. However, restoration greater than 1–2 km reconstructs a large area of mylonite with a more mafic Granite Mountain–type protolith in the source area of the Sunset Conglomerate (Fig. 3). Therefore our preferred estimate of ~1–2 km right-lateral strike-slip displacement across the Sunset fault is at the lower end of the plausible range. Greater dextral slip should have produced a mylonite-clast and Granite Mountain–clast-bearing conglomerate unlike the Sunset Conglomerate. This ~1–2 km right-slip estimate for the 10.8-km-long Sunset fault is less than that for the much longer San Felipe fault (5.8 ± 2.8 km) and is consistent with the Sunset fault being a short strand in a double stepover of the San Felipe fault zone.

Folds in and near the San Felipe Fault Zone

Folds deform all of the Cenozoic sedimentary rocks and some of the crystalline rocks in the study area (Fig. 3). We identified and analyzed this deformation in discrete structural domains and found that the directions and magnitudes of shortening vary across the area. There are five domains: (1) the folded Cretaceous mylonite at Yaqui Ridge, (2) the folded Late Cenozoic West Salton detachment fault, (3) folded Pleistocene Sunset Conglomerate, and (4 and 5) two domains of folded Pliocene sedimentary rocks near Yaqui Meadows (Fig. 13). We use structural analyses, map patterns, and shortening estimates from cross sections augmented by strain estimated from average interlimb angles to describe and compare folding trends, spacing, style, and strains in the three domains within the 9-km-wide Narrows stepover. We then compare folding patterns in the stepover with those in the remaining two domains of folded sedimentary rocks farther to the WNW in order to compare deformation related to the San Felipe fault zone with other folding strains.

We calculate horizontal shortening from cross sections and augment that data set by also calculating strain from the modal interlimb angles of folds (Table 1; Fig. 14). The interlimb method was used and tested by Kirby (2005) and Steely (2006). Shortened lengths were calculated from modal interlimb angle in two domains after approximating the folds there as one larger kink fold with one interlimb angle (Fig. 14). Folds may have a kink-fold geometry or a cylindrical geometry as long as fold limbs have fairly uniform orientations. Field data (Figs. 5, 6, and 13) indicate regular fold spacing and geometries in this area, and permit this simplification if two-fold limbs are clear in the stereogram, as they are at Yaqui Ridge (Fig. 12). In places where we

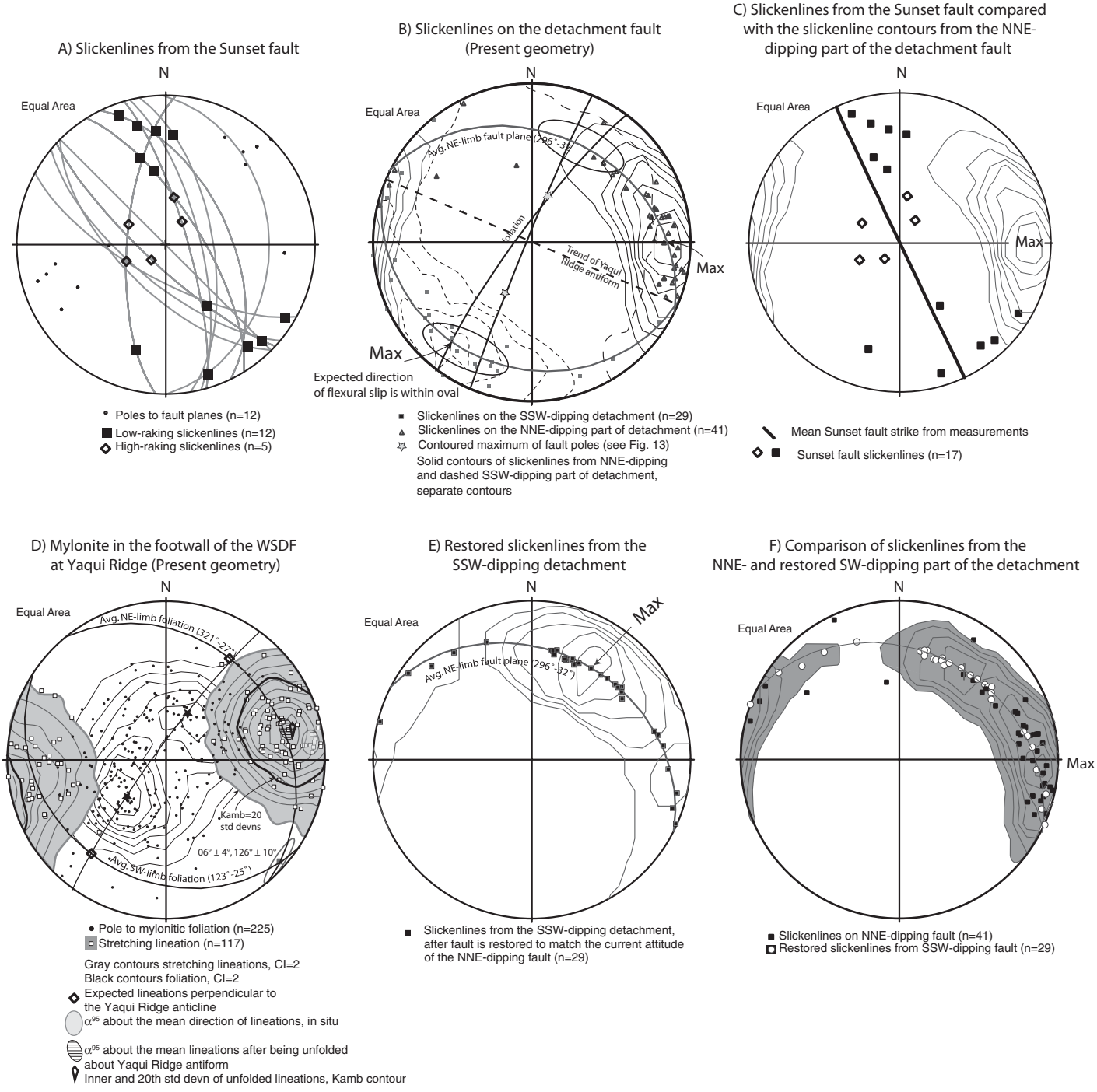

Figure 12. Geometry and kinematics of the Sunset and West Salton detachment faults (WSDF). (A) Slickenlines on the Sunset fault display significant scatter with more strike-slip and oblique vectors than dip-slip vectors. Note the variable dip direction of the Sunset fault. (B) Present-day geometry of the West Salton detachment fault, associated slickenlines, and fold axis. (C) Notice that strike-slip vectors on the Sunset fault do not have corresponding slickenline populations on the WSDF. This suggests that the Sunset fault was not kinematically linked to the WSDF and reactivation of the WSDF was limited or did not occur. (D) Scatter and contour plot of Cretaceous mylonitic foliations and stretching lineations in the footwall of the West Salton detachment fault. See text for discussion of unfolded data set. (E) Slickenlines from the SW-dipping part of the West Salton detachment after rotation to match the attitude of the detachment on the NNE-dipping part of the fault. The original attitude of the fault plane is not known. We restored the fault to a planar geometry in order to facilitate comparison of slickenline directions. Note the maximum Kamb contour in the NE quadrant. (F) Comparison of slickenlines directions on the NNE- and SW-dipping parts of the detachment fault. Note that slip in the 20° to 60° direction is far more common on the SW-dipping fault plane than on the NNE-dipping one. Slickenlines scattered around 90° are present on both parts of the detachment fault. Contour lines apply to slickenlines on both parts of the fault.

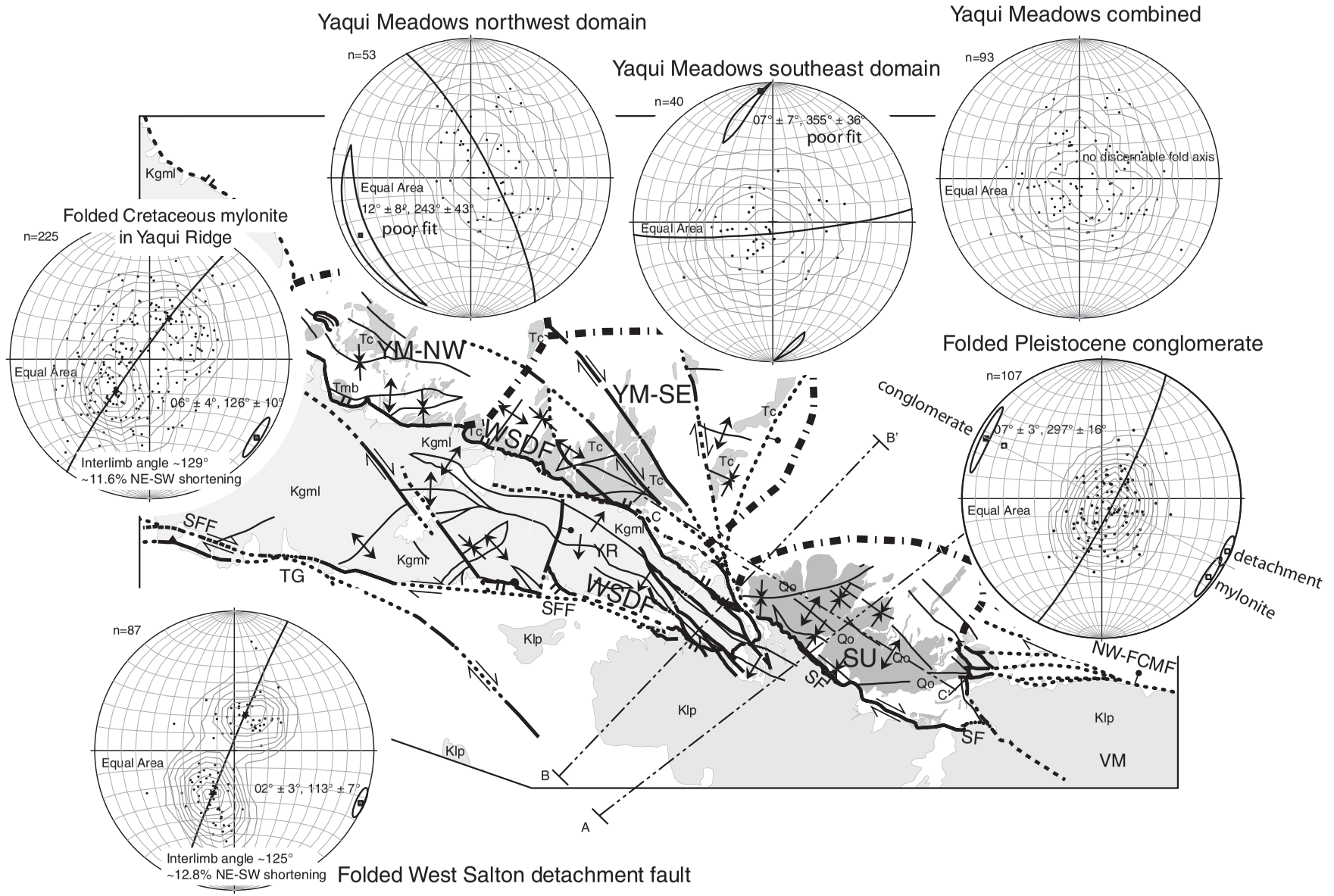

Figure 13. Simplified geologic map of the Yaqui Ridge area showing fold domains (dotted-dashed outlines) and their relationship to mapped fold traces and bounding faults of the San Felipe fault zone. Inset stereograms show individual fold domains and their interlimb angles where they can be determined. For each of three domains in the Narrows stepover, we compiled a best-fit cylindrical fold axis with its error oval in the SE quadrant of the stereonet depicting the folded Pleistocene sedimentary rocks in the Sunset domain. Note that all the rocks within the Narrows stepover zone of the San Felipe fault zone, from Cretaceous to Middle Pleistocene, are deformed about identically trending upright folds, within uncertainties. This trend is different from that in folds outside of the stepover and strongly suggests that the shortening in the stepover of the San Felipe fault zone is Quaternary. Data in Sunset and Yaqui Meadows domains are poles to bedding. NW-FCMF—Northwest Fish Creek Mountains fault; SF—Sunset fault; SFF—San Felipe fault; SM—Sunset Mountain; TG—Tamarisk Grove; VM—Vallecito Mountains; WSDF—West Salton detachment fault; YM-NW—Yaqui Meadows northwest domain; YM-SE—Yaqui Meadows SE domain; YR—Yaqui Ridge; YRF—Yaqui Ridge fault; SU—Sunset fold domain.

TABLE 1. STRUCTURAL ANALYSIS OF FOLDED ROCKS IN FIVE DOMAINS

Domain	Age of folded feature(s)	Fold-axis trend and plunge	Interlimb angle	NE-SW shortening from interlimb angle	NE-SW shortening from cross-section analysis
Yaqui Ridge footwall mylonite	Cretaceous	126° ± 10° 06° ± 4°	~129°	~11.5%	N/A
West Salton low-angle fault	Late Cenozoic	113° ± 7° 02° ± 3°	~125°	~13%	~11%–14%
Sunset Domain (Sunset Conglomerate)	Pleistocene	307° ± 12° 04° ± 2°	N/A	N/A	~7%–8% (~11%–12%)
Yaqui Meadows NE	Pliocene	243° ± 43° 12° ± 8°	N/A	N/A	N/A
Yaqui Meadows SW	Pliocene	355° ± 36° 07° ± 7°	N/A	N/A	N/A
Yaqui Meadows combined	Pliocene	No fold axis	N/A	N/A	N/A

Notes: Parentheses reflect addition of strain in angular unconformity. IL—Interlimb angle.

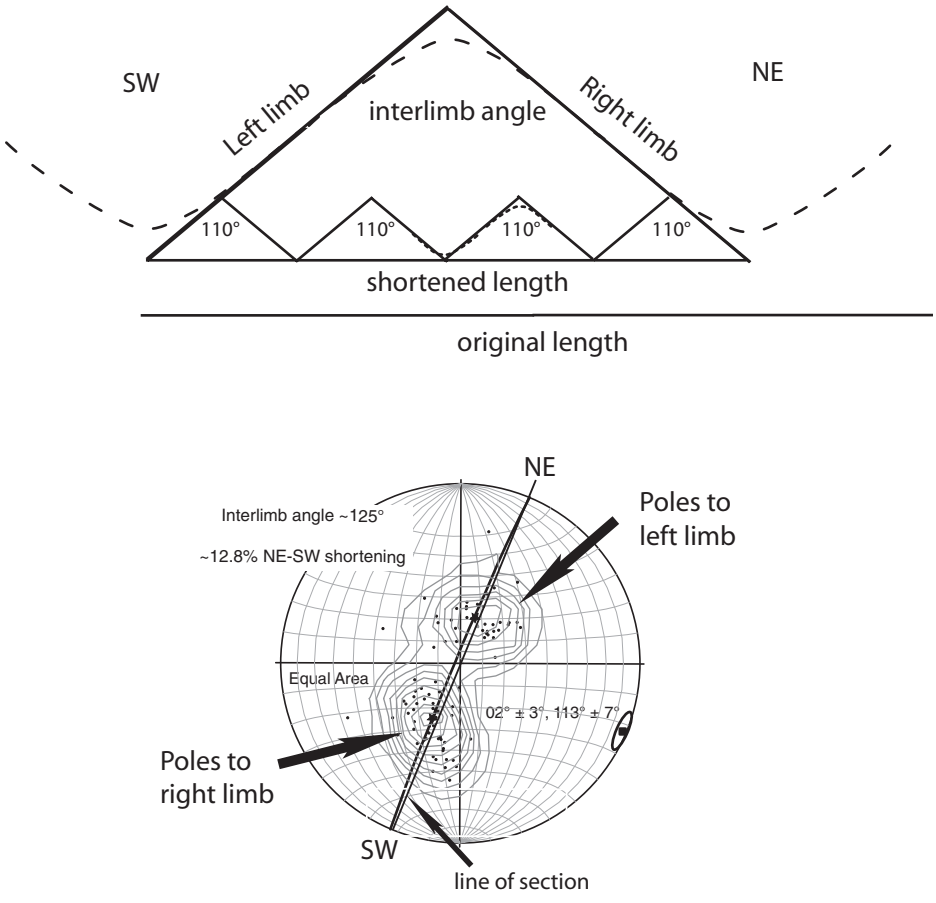

Figure 14. Technique to determine shortening strains from stereograms of folded bedding, faults, and foliation to augment cross-sectional analysis. Diagram shows that treating a group of small folds as a single larger fold is robust. Shortened length is calculated from modal interlimb angle in each domain. Folds may have a kink-fold geometry or a cylindrical geometry as long as fold limbs have fairly uniform orientations. Shortening calculated using modal dips of fold limbs and interlimb angles. Field data (Figs. 5, 6, and 13) indicate regular fold spacing and geometries in this area, and permit this simplification. Modified from Kirby (2005). Shortening calculated using a kink geometry is comparable to that calculated using a concentric geometry. Both types of folds are present.

can estimate horizontal shortening using both methods, there is good agreement between these two methods (Table 1; see below).

We also analyze mylonitic stretching lineations from the Cretaceous mylonite and slickenlines from the West Salton detachment fault to help constrain the timing, geometry, and mechanism of folding at Yaqui Ridge. Lineations on the NNE-dipping side of the antiform plunge ENE, whereas lineations on the opposite limb plunge W to WSW.

Folded Mylonite at Yaqui Ridge: Description and First-Order Analysis

This domain encompasses all the rocks in the footwall of the West Salton detachment fault along Yaqui Ridge. There, foliated to mylonitic plutonic rocks of the Eastern Peninsular Ranges mylonite zone and local lozenges of metasedimentary rocks define NW, NE, and E-W–trending folds (Figs. 5 and 13). Map analysis shows that WNW-trending folds are dominant with fewer short E-W–trending and ENE-trending folds (Fig. 5). Along most of Yaqui Ridge, two monoclines define an antiformal box fold with hinges 300–600 m apart. These monoclines generally parallel the West Salton detachment fault on the N flank of Yaqui Ridge, define the crest of the antiform in the footwall, and are ~0.25 km SSW of the detachment fault (Fig. 5). The San Felipe fault zone also parallels the monoclines.

The monoclines change northwestward into anticlines in an area where several smaller synclines merge with and link the major anticlines. One of the dominant NW-trending anticlines dies out to the NW, whereas the other NW-trending anticline changes orientation and may be continuous with the NE-trending anticline that intersects the San Felipe fault zone at the boundary between the Pinyon Ridge and Mescal Bajada structural segments (Figs. 5, 6, and 13).

Our mapping of fold axes and structural analysis of 225 foliation measurements shows that ESE-plunging folds dominate Yaqui Ridge (Figs. 5, 7, 12, and 13). The best-fit cylindrical fold plunges 06° ± 4° and trends 126° ± 10°. The dominant ESE plunge of the folds is probably due to the original easterly dip of the Cretaceous thrust-related fabrics. The NE- and E-trending folds are not evident in the stereonet in part because fewer attitudes were collected where these folds dominate. Cross folds may contribute to some of the dispersion in the data set but do not obscure the dominant pattern.

The lack of a distinct marker unit in the mylonite precludes a rigorous cross-sectional analysis of shortening. Although data are scattered, an interlimb angle of ~129° is measured from the contoured center of poles to each fold limb (Figs. 13 and 14). The interlimb angle in this

domain yields ~11.5% NE-SW shortening of the mylonite across Yaqui Ridge (Table 1). An original NNE- to ENE-dipping mylonite zone is likely, given regional relationships, but this dip direction is not required for the strain calculation (see below).

Stretching lineations in the mylonite show a strong ENE-trending population on the NE-dipping limb, and a WSW-trending population on the opposite limb (Fig. 12D). The lineations are neither parallel nor perpendicular to the Yaqui Ridge antiform.

Folded West Salton Detachment Fault: Description and First-Order Analysis

We analyzed the antiformal geometry of the West Salton detachment fault along the NE and S sides of Yaqui Ridge (Figs. 5, 6, 7, and 13). At the SE tip of Yaqui Ridge, E of the Narrows, NE-dipping, SE-dipping, and SW-dipping parts of the West Salton detachment fault define an ESE-plunging box-shaped antiform (Figs. 5 and 6). This box fold is coincident with the box fold defined by the foliations in the underlying footwall at map scale and indicates that either the mylonite and detachment fault were folded during the same event, or the detachment fault reactivated a preexisting box-shaped antiform in the Cretaceous mylonite zone. The ESE plunge of the fold in the detachment fault is likely inherited from the original ENE dip of the West Salton detachment fault, based on its consistent easterly dip along its ~150 km trace length (Todd et al., 1988; Axen and Fletcher, 1998).

Stereonet analysis of 87 fault-plane measurements show two limbs that define a 02° ± 3°–plunging, 113° ± 7°–trending fold axis (Figs. 13 and 14). Measurement of horizontal NE-SW shortening calculated from two cross sections shows that the West Salton detachment fault was shortened by ~11.5%–14.0% across Yaqui Ridge (Fig. 7; Table 1). An interlimb angle of 125° is measured from the contoured poles to the detachment on the north and south side of Yaqui Ridge. We calculate ~13% NE-SW shortening of the detachment fault across Yaqui Ridge, and by assuming that the detachment fault was nearly planar and dipping before folding. Unfolding was done about the axis of the Yaqui Ridge antiform. This second method of strain analysis does not require that we know the original orientation of the fault near Yaqui Ridge, merely that it was nearly planar before folding. Within errors, the shortening of the detachment fault measured from the cross section and calculated using the interlimb method is identical. Both methods produce the same direction and magnitude of shortening as that recorded in the folded Cretaceous mylonite (Fig. 13; Table 1).

Slickenlines from the NNE-dipping detachment fault preserve scattered slickenlines concentrated around a top-east direction, whereas the SW-dipping detachment fault has greater dispersion with a SW-trending maximum and scattered slickenlines elsewhere (Fig. 12C). The many SW-plunging slickenlines on the SW-dipping part of the fault require transport of the hanging wall up and over Yaqui Ridge and are geologically implausible slip directions for the detachment fault in its current geometry. When the SW-dipping detachment fault and its slickenlines are restored about the Yaqui Ridge antiform (Fig. 12E), many scattered slickenlines rotate to congruence with the E-trending maximum on the NNE-dipping part of the detachment fault (Figs. 12C, 12E, and 12F) as predicted, if the detachment fault was folded after these E-plunging slickenlines formed. We interpret these data as evidence for folding of the detachment fault and the underlying mylonite after the top-to-the-E detachment slip. The E-trending maximum defines the dominant slip direction across the detachment fault, and is evidence for highly oblique dextral-normal slip across the West Salton detachment fault at Yaqui Ridge (Steely et al., 2004; Steely, 2006).

When slickenlines from the two limbs are compared (Figs. 12C and 12F), it is clear that the two limbs preserve different slip histories, in addition to sharing a population of E-plunging slickenlines that range from ENE to ESE. Over 80% of the slickenlines on the NNE-dipping part of the fault are in the E-plunging population, as are a third of the slickenlines from the SW-dipping parts of the detachment fault (Fig. 12F). The remaining slickenlines are located in the middle of the NE or SW quadrants. This population is far more abundant on the SW-dipping limb in either its restored geometry (Figs. 12E and 12F) or its current geometry (Fig. 12C). We interpret the populations of slickenlines as evidence that both parts of the fault experienced top-to-the-E displacement, whereas NE-directed slip was limited largely to the SW-dipping part of the fault.

Folded Quaternary Sedimentary Rocks: Description and First-Order Analysis

The Sunset domain exposes NW-striking Pliocene to Quaternary sedimentary rocks between the Sunset fault and the Fish Creek Mountains fault (Figs. 6 and 13). Map analysis shows that folds in the Sunset Conglomerate have two orientations. There is a dominant set of WNW-plunging folds in the central part of the domain, and a subordinate pair of E- and W-plunging monoclines at the N and south ends of the domain (Fig. 6). Overall, there are four to five NW-plunging folds parallel to and within ~1.5 km of the Sunset fault. The central anticline in this domain is offset in a left-stepping sense by NE-striking left-lateral faults (Fig. 6). Together the folds transform a 1.7-km-wide, SW-dipping homocline in the WNW into a 1.25-km-wide, NE-dipping homocline in the ESE.

When the attitude of bedding of Pleistocene beds in the Sunset domain are analyzed (n = 107), stereonet analysis shows an overall 07° ± 3°–plunging, 297° ± 16°–trending, cylindrical fold axis. This direction is parallel to the nine fold hinges that we mapped (Fig. 6) and parallel to both the Sunset fault and the Fish Creek Mountains fault (Fig. 13). There is somewhat more scatter in this data set than in some of the other domains due to the greater measurement error associated with the bedded conglomerate and pebbly sandstone. Cross-section analysis of the Sunset domain shows a minimum of ~7%–8% NE-SW horizontal shortening (Fig. 7; Table 1). The 10°–15° NE-dipping angular unconformity at the base of the Sunset Conglomerate may represent an additional ~3.5%–4% NE-SW shortening that occurred before deposition of the Sunset Conglomerate for a total NE-SW shortening of ~11% to ~12% (Table 1).

Folded Sedimentary Rocks outside the San Felipe Fault Zone at Yaqui Meadows: Description and Analysis

There are two areas of folded Canebrake Conglomerate of the Pliocene Palm Spring Group in the hanging wall of the West Salton detachment fault along the NNE side of Yaqui and Pinyon Ridges that we named the NW and SE Yaqui Meadows domains (Fig. 13). These rocks are located west of the Narrows stepover in the San Felipe fault zone and are cut by the distal ends of the Sunset fault zone. Mapping of the NW Yaqui Meadows domain revealed mostly W-plunging folds (Fig. 5). The SE Yaqui Meadows domain also preserves E-W–trending folds and at least three NNE-plunging folds at a high angle to the West Salton detachment fault (Figs. 5 and 13). The detachment fault is not folded about these NNE-plunging axes and probably acted as a décollement surface during the folding.

The NW Yaqui Meadows domain shows significant scatter of bedding attitudes on a stereogram with no meaningful fold axis evident on the stereonet despite the presence of several clear mapped folds (n = 53) (Fig. 13). The SE Yaqui Meadows domain also shows a significant scatter of bedding attitudes (n = 40) (Fig. 13).

When the attitudes from the NW and SE Yaqui Meadows area are combined, bedding attitudes display significant scatter with no dominant fold axis on the stereogram (Fig. 13). This is likely due to interference between the multiple trends of folds at high angles to one another.

E-W–trending folds near Yaqui Meadows probably reflect wrench deformation. We have not identified a mechanism to produce the handful of NE-plunging folds in the area. It is noteworthy that there is no evidence for NW-trending folds in either the map pattern or the stereogram around Yaqui Meadows. NW-trending folds are localized between en echelon faults of the San Felipe fault zone.

INTERPRETATION AND DISCUSSION

Timing of Initial Uplift along the San Felipe Fault Zone

The northeastward tilt of older sedimentary rocks beneath the angular unconformity at the base of the Sunset Conglomerate and the lack of Borrego or Hueso Formations across this contact indicate a period of uplift and tilting prior to deposition of the basal Sunset Conglomerate. Because our study area is astride a poorly understood paleogeographic boundary between the thicker Borrego-filled subbasin to the north (up to 1.8 km thick) and the thinner Hueso-filled subbasin to the south (~1.3 km thick), it is impossible to know the thickness of Hueso- or Borrego-age sediment missing across the angular unconformity. Using reasonable exhumation rates of 2–10 mm/yr and complete erosion of the maximum possible thickness of Hueso or Borrego Formation, ~0.1–0.9 m.y. would be required to erode these units before deposition of the Sunset Conglomerate began. Alternatively, if the Borrego or Hueso Formations were thin or absent in this area, then the unconformity could have formed over a period of <0.1 m.y. This analysis does little to constrain the age of initial deformation because we cannot estimate the thickness of the Borrego or Hueso Formations near Yaqui Ridge.

Therefore, we examined basin fill for evidence of the earliest uplift along the SW margin of the San Felipe–Borrego subbasin. Rare recycled sandstone clasts in conglomerate of the upper Borrego Formation (95 m below the base of the Ocotillo Formation) in the southwestern Borrego Badlands provide the earliest record of basin inversion and uplift along the SW basin margin. Although the rate of sediment accumulation in the upper Borrego Formation is not well known, it is likely less than the high rates in the lower Ocotillo Formation (1.4–3.9 mm/yr) (Lutz et al., 2006; Kirby et al., 2007). Using a reasonable range of sediment-accumulation rates (0.5–2 mm/yr), the ~100 m thickness of upper Borrego Formation with recycled clasts, and the ca. 1.1 Ma age of the basal Ocotillo Formation in the Borrego Badlands where the basal contact is conformable (Lutz et al., 2006), the oldest recycled clasts were probably deposited ca. 1.1–1.3 Ma. These recycled clasts record erosion of quartz-rich sandstone from either the Diablo or the lower Borrego Formations and provide the earliest evidence of uplift and erosion within the future San Felipe fault zone. Aside from this one conglomerate bed in the Borrego Formation, there is currently no other sedimentary evidence for uplift along the SW margin of the San Felipe–Borrego subbasin prior to 1.1–1.3 Ma.

We interpret these data as evidence that there was little or no uplift in the San Felipe fault zone prior to deposition of the uppermost Borrego or lower Ocotillo Formation. We further infer that the lag time between initiation of the San Felipe fault (which inverted and destroyed some of the older supradetachment basin) and earliest deposition of reworked sandstone clasts in the new basin was probably <0.2 m.y. The close spatial association between the uplifted areas in the Vallecito and Fish Creek Mountains and the San Felipe fault zone provides evidence that the San Felipe fault zone produced the uplift. Altogether these relationships show that the San Felipe fault zone initiated no earlier than ca. 1.1–1.3 Ma and breached the surface shortly afterward.

Geometry of Initial Uplift along the San Felipe Fault Zone

Northeastward tilt of rocks beneath the Sunset Conglomerate prior to deposition of the Sunset Conglomerate, and the location of the uplifted area adjacent to the San Felipe fault zone, are consistent with growth of a NE-facing fault-propagation monocline above the nascent, upward-growing tip of the Sunset and Fish Creek Mountains faults. A fault-propagation fold above a dextral-oblique fault will produce uplift during early stages of development, similar to a fault-propagation fold above a growing reverse or normal fault (Gawthorpe et al., 1997; Sharp et al., 2000). Once the fault tip reaches the surface, accommodation space is quickly created on the downthrown side of the fault (in this case the NE side), and deposition begins (Gawthorpe et al., 1997). Although the San Felipe fault zone is predominantly a strike-slip fault, it has a significant NE-side–down component of slip in the Narrows stepover and along the Fish Creek Mountains fault and a smaller component of SW-down slip on the Pinyon Ridge structural segment (Dibblee, 1996; Steely, 2006). A fault-propagation fold above the Sunset fault can explain uplift and erosion of Plio-Pleistocene basin fill (Diablo, Borrego, and/or Hueso Formations) shortly prior to deposition of the basal Sunset Conglomerate. This model also explains the original NE dip of older basin-fill deposits beneath the angular unconformity below the Sunset Conglomerate. A second, SW-facing monocline associated with the E end of the San Felipe fault at Yaqui Ridge may have formed in a similar manner, but sedimentary evidence for such an evolution is not preserved there.

The Sunset fault may cut the West Salton detachment fault at depth or merge laterally and at depth with it. We prefer the first interpretation because other faults of the fault zone, such as the San Felipe fault, cut and offset the detachment along San Felipe Wash by many kilometers, and because small-offset dextral strike-slip faults between the San Felipe and Sunset fault cut the West Salton detachment fault near the tip of Yaqui Ridge. Both relationships show that dextral faults cut the detachment fault instead of reactivating it (Figs. 3 and 5). Second, there is no Ocotillo Formation in the hanging wall of the detachment fault north of Yaqui Ridge as would be expected if it was active during the first half of the San Felipe fault zone's history. Finally, the two faults have dissimilar dominant slip directions and the faults are nearly orthogonal where they are closest to each other (Fig. 7C). The slip vectors measured on the Sunset fault, although few in number, are distinctly different from major slickenline population on the West Salton detachment fault (Figs. 12B and 12C). Sunset fault slickenlines overlap in trend with less than 6%–7% of slickenlines on all parts of the detachment fault, and overlap even less with slickenlines on the nearest part of the detachment on the north side of Yaqui Ridge (Fig. 12B).

These relationships conflict with an alternate possibility, that there was some folding and uplift of basin fill during late stages of slip on the West Salton detachment fault, before the San Felipe fault was fully formed. We do not favor this alternate model because the San Felipe fault zone clearly cuts the detachment fault and was active long enough to accumulate significant right slip. Syndetachment tilting should have been toward the detachment fault (to the SW) rather than the observed dip direction beneath the angular unconformity (to the NE). In addition, the detachment fault was active during all of Pliocene time yet did not produce a Pliocene uplift within the future San Felipe fault zone.

Age of the Sunset Fault and Paleogeography of the Sunset Conglomerate

Our data show that the Sunset and Fish Creek Mountains faults controlled deposition of the Sunset Conglomerate along the SW margin of the newly formed San Felipe–Borrego subbasin of the Salton Trough (Fig. 11). Based on correlation to more distal, well-dated parts of the Ocotillo Formation (Lutz et al., 2006; Kirby et

al., 2007), the oldest Sunset Conglomerate is estimated to be ca. 1.1 ± 0.2 Ma. We infer that the Sunset fault had ruptured to the surface by that time, was creating accommodation space, and had cut the detachment fault. Our data also show that the Sunset Conglomerate accumulated in a syntectonic alluvial fan with sedimentary transport to the NE away from the bounding San Felipe fault zone.

Emergence of the San Felipe fault zone records a major, structurally controlled change in the paleogeography of the San Felipe–Borrego region from one controlled largely by oblique low-angle extension across the West Salton detachment fault to one dominated by strike-slip faults (Figs. 11A and 11B). The presence of clasts recycled from the Palm Spring Group requires uplift and erosion of older basin-fill deposits SW of the Sunset fault and erosion of the Palm Spring Group from newly uplifted highlands in the proto-Vallecito Mountains and proto-Fish Creek Mountains. The absence of the Borrego and Hueso Formations, coupled with the angular unconformity beneath the Sunset Conglomerate, suggests that NE tilting or folding accompanied this uplift event. The deposits of the Palm Spring Group that once covered the plutonic mountain core have been stripped by erosion since the early Pleistocene. Initiation of the San Felipe fault zone inverted and eroded parts of the basins of the western Salton Trough and caused crystalline-cored fault blocks (the Vallecito and Fish Creek Mountains) to emerge from beneath the sedimentary floor of the basin. Our work supports the original hypothesizes of Kirby (2005), Lutz et al. (2006), and Kirby et al. (2007) (Fig. 11).

Origin of the Yaqui Ridge Antiform

Several hypotheses (in end member or in combination) can plausibly explain the folded form of the Cretaceous mylonite and detachment fault at Yaqui Ridge (Figs. 6, 7, and 13): (1) the original folded form of the mylonite could date back to Cretaceous thrusting and be an original corrugation that was reactivated by the West Salton detachment fault; (2) folding may be entirely or partially syndetachment faulting; and/or (3) the fold could result entirely from deformation within the San Felipe fault zone. For clarity we restrict our discussion of the antiform's origin to the process that generated opposing dips, and we do not address whether departures from regional strike of the detachment fault and/or its underlying mylonite zone are original or secondary. Comparison of the NE-dipping mylonite at Yaqui Ridge with regional trends (Sharp, 1967) suggests that its strike is slightly counterclockwise of the mylonite farther north. This is due to some original waviness in the mylonite zone and/or anticlockwise rotation.

Hypothesis 1: Folding during Cretaceous Thrusting

If the antiformal shape of the mylonite at Yaqui Ridge is a primary feature that formed during Cretaceous thrusting, then it must be possible for the slickenlines on the West Salton detachment fault (which effectively reactivated the Cretaceous mylonite) to have formed and been active in their current orientation. In addition, stretching lineations in the Cretaceous mylonite on both antiformal limbs should record a feasible thrust-related direction of slip in present-day coordinates, and so are most likely to align either down the nose of the Yaqui Ridge antiform or be perpendicular to it. Other orientations of the mylonitic lineation are less likely because high strains of sheath folds and triclinic folds are not evident, and the antiform is in the wrong orientation to be a thrust ramp (see below). In an original Cretaceous corrugation, a tighter clustering of mylonitic stretching lineations is expected in present coordinates than if we structurally "unfold" the antiform. If unfolding the foliation about the Yaqui Ridge antiform improves the clustering of the lineations, then folding of the mylonitic fabric probably occurred after the lineations formed in the Cretaceous.

The above tests show that creation of the Yaqui Ridge antiform in the Cretaceous during thrusting is very unlikely. Most importantly, the slickenlines on the West Salton detachment fault could not have formed on a detachment with an original antiformal shape. Improbable reverse-sense slip is required on the detachment by this interpretation during the time when the top-to-the-E– and top-to-the-NE–trending slickenlines were produced on the SW-dipping part of the detachment fault. Second, transport in the mylonite, as recorded in the top-to-the-WSW–stretching lineations, is neither perpendicular to the Yaqui Ridge antiform, nor parallel to the antiform (Fig. 13). The oblique angle between the antiform and the lineations requires a complex, triclinic origin such as sheath folding or formation of an oblique thrust-related ramp that dips in the transport direction, if the observed geometries are original and Cretaceous. A thrust ramp with such a dip direction is improbable. Third, the stretching lineations define a good cluster in their current orientations (Fig. 13) but restore to a significantly tighter congruent cluster after unfolding of the mylonitic fabric about the Yaqui Ridge antiform. Currently the 20-sigma Kamb contour of the lineations spans ~130° of the net's 180° width, and the modal direction of the Kamb contour does not overlap the mean vector at the α_{95} level. Unfolding the stretching directions about the Yaqui Ridge antiform produces a population that is more clustered. The 20-sigma Kamb contour of the unfolded lineation spans ~85° of the net, and there is an excellent overlap of the modal Kamb direction and the mean vector (α_{95} = 4.4°). The geometry of the mylonitic lineations is more consistent with folding of the mylonite after Cretaceous time, but the lineations alone do not require it. Fourth, preliminary paleomagnetic studies show post-mylonitic tilting and folding in the Yaqui Ridge antiform, and are inconsistent with the antiform being an original corrugation (B. Housen, 2002, 2007, written commun.). All in all, the simplest interpretation is to fold all the structural elements after Cretaceous time during a single period of folding and faulting.

Hypotheses 2 and 3: Syndetachment versus Postdetachment Folding

Our mapping shows that folds in the mylonite at Yaqui Ridge and the folded detachment fault in the left stepover between the San Felipe fault and the Sunset fault have geometries nearly identical to those of folds in the Pleistocene Sunset Conglomerate in the adjacent stepover between the Sunset and Fish Creek Mountains faults (Figs. 5, 6, and 12). Fold axes reflect identical NE-SW–shortening directions, and fold hinge lines have similar spacing. Cross folds, at an angle to the dominant trend, are present but subordinate in both stepovers. Folds within the stepovers of the San Felipe fault zone have a much more consistent shortening direction (NE-SW) than folds that formed outside the Narrows stepover near Yaqui Meadows (weak N-S) (Fig. 13). Folds within the San Felipe fault zone consistently trend WNW to NW, and represent roughly 10 ± 3% NE-SW horizontal shortening.

Despite some scatter in the stereonets of bedding attitudes, it is clear from the map patterns and fold analyses that the trend of the dominant folds that deform the Pleistocene Sunset Conglomerate is identical to the trend of the Yaqui Ridge antiform (Figs. 3 and 13). Plunge directions differ, however. We infer that the WNW plunge of the folds in the Sunset Conglomerate is due to northwestward tilting of the Sunset Conglomerate toward a SE-dipping normal fault buried along San Felipe Wash (Figs. 7C and 13). The ESE plunge of the folded Cretaceous mylonite and the detachment fault is inherited from the original easterly dip of these features, as noted above.

The total amount of NE-SW horizontal shortening is about a third greater in the Yaqui Ridge antiform than in the Pleistocene Sunset

Conglomerate (Table 1). The difference in strain could reflect spatial or temporal differences in strain, or both. There might be more accumulated strain in the stepover between the San Felipe fault and the Sunset fault than in the second stepover between the Sunset fault and the Fish Creek Mountain fault. Variations in the fault geometry could produce modest differences in folding strains in adjacent stepovers of a single fault zone. Alternatively, the "extra" strain in the crystalline rocks could have been created by: (1) initial deformation in the San Felipe fault zone before or during deposition of the Sunset Conglomerate; (2) a small-magnitude antiform inherited from the Cretaceous mylonite zone; and/or (3) a small-magnitude antiform created during slip on the West Salton detachment fault.

If we add the ~3.5%–4% NE-SW shortening reflected in the NE-tilted angular unconformity beneath the Sunset Conglomerate to the shortening from the cross section of the Sunset Conglomerate, there is no significant discrepancy in the amount of shortening between the two adjacent stepovers (Table 1). The additional strain is late Pliocene to Pleistocene and strongly suggests that initial deformation in the San Felipe fault zone started before deposition of the oldest Sunset Conglomerate ca. 1.1 ± 0.2 Ma, and that little or none of the folding dates back to Cretaceous thrusting.

Because most of the shortening is preserved as folds in the Pleistocene Sunset Conglomerate, roughly two-thirds of folding occurred after the end of conglomerate deposition, that is, after ca. 0.6 Ma. The angular relationships across the unconformity (Figs. 5 and 6), however, are consistent with a continuum of NE-SW shortening and transpression beginning before deposition of the oldest preserved Sunset Conglomerate. Thus folding of the Sunset Conglomerate is likely the result of persistent NE-SW shortening. NE-SW contraction started before deposition of the basal Sunset Conglomerate, was ongoing during deposition of the conglomerate, persists to the present, and is currently exhuming the conglomerate. We did not directly observe growth strata in the Sunset Conglomerate, in part due to discontinuous exposures, but we infer that they are present.

Based on the above summary, we favor an interpretation in which the Sunset Conglomerate, the Cretaceous mylonite on Yaqui Ridge, and the West Salton detachment fault experienced a single episode of shortening in the double left stepover of the San Felipe fault zone, rather than representing multiple deformational events. Our data and analyses do not preclude some SW tilting of the south limb of the Yaqui Ridge antiform during the latest stages of detachment faulting, but we emphasize that it must be a small portion of the overall tilt. Folds in the stepover were produced by transpressional strain transfer across the 9-km-wide contractional left-step in the San Felipe fault zone. These two contractional stepovers provide a soft link between the Mescal Bajada segment of the San Felipe fault, the Sunset fault, and the WNW end of the Fish Creek Mountains fault. We infer that the San Felipe fault zone may be a continuous structure in the subsurface, however, and that the double left step and WNW-trending folds at the present level of exposure are all part of a complex flower structure that developed structurally above a continuous or nearly continuous fault zone. A flower structure explains the strong parallelism between fold axes in the stepover zones and the strike of the en echelon dextral faults, a parallelism that is difficult to explain with wrench fault models. Fault-bend folding in a three-dimensional flower structure is more likely to explain the parallelism of the folds and faults than strain partitioning because the available slickenline data on the San Felipe fault zone are inconsistent with strain partitioning between faults.

Other models for the origin of folds at Yaqui Ridge and in the Sunset Conglomerate are not favored because they do not predict the observed fold geometries; they are inconsistent with the strong spatial association of the WNW- to NW-trending folds with the more contractional segments and stepovers in the San Felipe fault zone. Extensional folding processes are very unlikely to explain these NW-trending folds because extensional processes rarely produce the observed trains of folds or such complex, locally interfering three-dimensional fold patterns (e.g., Janecke et al., 1998; 2005a). The presence of four to five closely spaced folds in a fold train parallel to the Sunset fault, within a large left-stepping contractional stepover in a major regional strike-slip fault zone, is difficult to explain with extensional fold models. We also reject wrench folding as a viable mechanisms because it predicts that most fold axes would trend E-W, oblique to the bounding faults rather than parallel to them. Folding and faulting in the Sunset Conglomerate and at Yaqui Ridge is the result of contraction and fault-bend folding within two left steps in the right-lateral San Felipe fault zone, and of contraction north of the E-striking segments of the San Felipe fault.

In summary, our data suggest that the majority of folding across the Yaqui Ridge antiform and in the Sunset Conglomerate domain occurred as a result of oblique transpression within a major double left step and restraining bend in the San Felipe fault zone. Folding probably started just prior to deposition of the Pleistocene Sunset Conglomerate, with the bulk of shortening occurring during and after deposition of the youngest preserved beds. Although a low-amplitude original corrugation and/or slight folding during detachment faulting are permitted by the data, a single folding event in the Quaternary provides a simpler explanation.

Evidence for Flexural Slip Folding in the Yaqui Ridge Antiform

Slickenline data from the West Salton detachment fault are complex and show a large dispersion around a modal top-to-the-east slip direction (Fig. 12C). This top-to-the-east population is present on both limbs of the Yaqui Ridge antiform. The current antiformal shape of the detachment is not geologically plausible during slip across it, however. It would require the impossible—that the hanging wall of the detachment fault had reverse-sense slip across the SSW-dipping part of the detachment fault when both the E- and NE-trending slickenlines were forming. Such slip can develop easily, if there is a breakup fault or secondary breakaway to the back tilted part of the detachment fault. However, our multi-university research group has identified no such fault near Yaqui Ridge in the seven years of detailed mapping. Large expanses of the hanging wall demonstrably do not have such a structure (Steely, 2006; Janecke, unpublished mapping). Altogether the lineation and slickenline data show that the Yaqui Ridge antiform (the detachment fault and the underlying mylonite) cannot be an original corrugation or fold that predates slip across the detachment fault. The mylonite was likely much more planar but dipping prior to folding.

During folding of an originally NE- (?) to ENE-dipping mylonite and West Salton detachment fault to its current symmetric antiformal geometry, there must have been greater reorientation and tilting of the SW-dipping limb than of the NE- or N-dipping limb. A symmetric antiform would result from monoclinal folding of originally dipping features. In effect, the Yaqui Ridge antiform has one tilted limb, like a monocline, not two tilted limbs, like an anticline. Significant northeastward tilting of the NE-dipping part of the detachment fault is unlikely because the fault has such a low dip (Figs. 2, 7, and 13).

It is striking that the incongruent dip-slip slickenlines that are so numerous on the SW-dipping part of the West Salton detachment fault (Figs. 12C, 12E, and 12F) are distributed in a plane perpendicular to the axis of the Yaqui Ridge antiform (113° ± 7° and 126° ± 10°). We suggest that these dip-slip slickenlines on the SW-dipping part of the detachment fault formed during flexural slip across the fault plane within

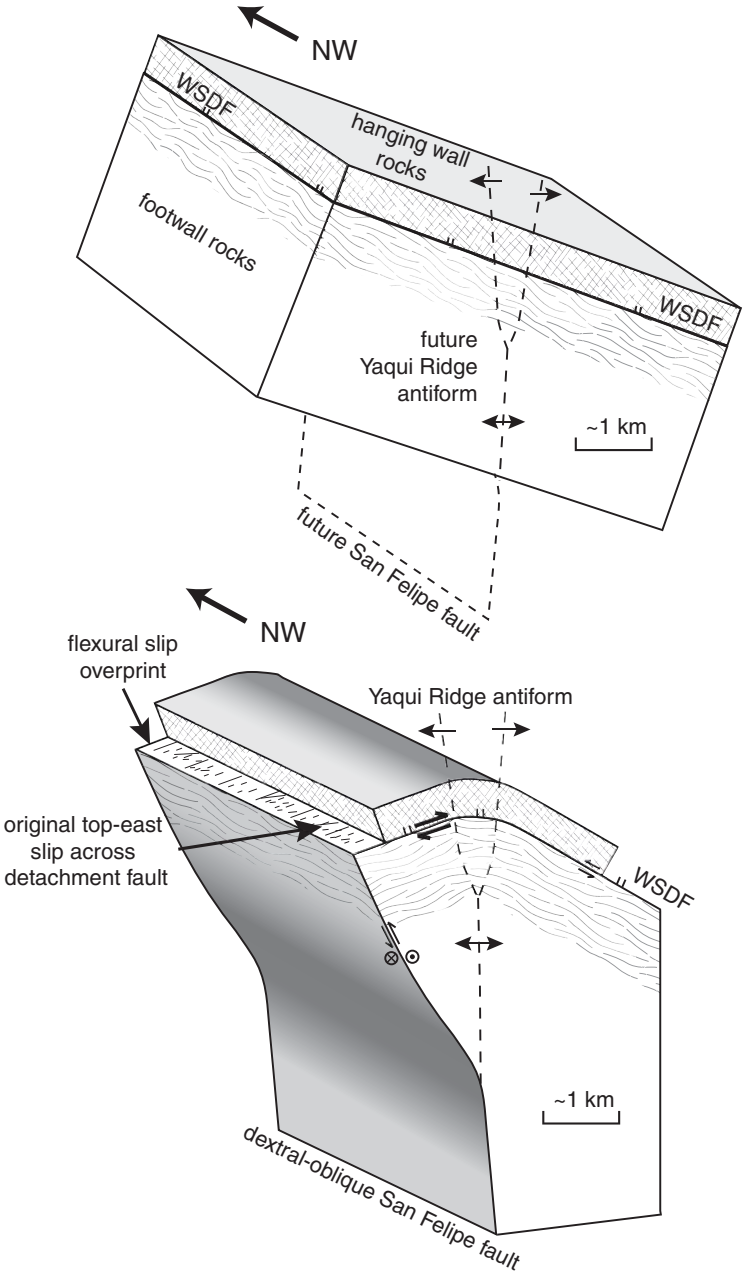

Figure 15. Schematic diagram showing the formation of slickenlines due to flexural slip between the hanging wall and footwall of the West Salton detachment fault (WSDF) during younger monoclinal folding. Note that formation of the Yaqui Ridge antiform is the result of a SW-dipping monocline that deformed an originally NNE- to ENE-dipping mylonite and detachment fault.

a growing, SW-facing monocline (Fig. 15), in a manner originally suggested by Axen and Fletcher (1998) to explain disparate slip indicators reported by Stinson and Gastil (1996) farther south along the detachment fault. The east-northeastward regional dip direction of the detachment fault and this monocline model predict that there was less reorientation and flexural slip across the NE-dipping part of the detachment fault, and therefore many fewer NE-plunging dip-slip slickenlines are expected there. This prediction agrees with the data (Fig. 12). Seventeen percent of the slickenlines on the NE-dipping part of the detachment lie near the center of the NE quadrant, whereas 80% of the slickenlines on the SW-dipping limb have this dip-slip trend and are perpendicular to the antiform (Figs. 12 and 15) (Steely, 2006). The 90° angular difference between the WNW trend of the Yaqui Ridge antiform and the SW-plunging slickenlines SW of the antiform is the difference predicted by the monoclinal flexural-slip model (Fig. 12C). Crosscutting relationships between NE- and E-trending slickenlines are not preserved within the fault zone, so it was not possible to further test our hypothesis by assessing whether NE-trending slickenlines are younger than the E-trending ones.

In summary, our data show that the footwall mylonite and West Salton detachment fault at Yaqui Ridge have an antiformal shape that cannot be attributed to an original corrugation of the Cretaceous mylonite, folding of the mylonite before detachment slip, or folding of the detachment fault and mylonite during slip on the detachment fault. Regional relationships and our structural analysis suggest that the mylonite and detachment fault were originally NNE- to ENE-dipping and much more planar before the early Pleistocene, although their predeformational strike may have departed somewhat from regional trends. A SW-facing monocline explains the antiformal shape of an originally ENE- to NNE-dipping mylonite and detachment fault at Yaqui Ridge. Flexural slip along the detachment fault during folding in the Narrows stepover can produce the anomalous dip-slip population of slickenlines (NE- and SW-plunging) that are more abundant on the SW-dipping part of the detachment fault than on the NNE-dipping part of the fault. We therefore document two monoclines along the San Felipe fault zone: a short NE-facing monocline that probably formed above the upward propagating NE-side down Sunset fault and a longer SW-facing monocline near the San Felipe fault.

Deactivation of the West Salton detachment fault and the duration of temporal overlap with the San Felipe fault zone

We initiated this study in part to determine if the initiation of dextral faults SW of the southern San Andreas fault quickly deactivated the older West Salton detachment fault (abrupt episodic behavior) or if there was a large demonstrable overlap in activity on the two fault systems (more complex evolving behavior). The answer to this question would indicate when the West Salton detachment fault was last active as a single, ~125-km-long structure that was continuous from Palm Springs in the north to the Vallecito–Fish Creek basin in the south. The distinction between slip on a coherent detachment fault and continuing slip on much smaller parts of the detachment is important because

the tectonic and basinal implications of these two contrasting modes are very different. In the former case (coherent detachment fault), the entire western Salton basin would continue to subside, whereas the second mode would allow continued slip on parts of the detachment coeval with new, younger structures. This should produce localized uplifts and basins as the original supradetachment basin was partly dismembered by dextral faults.

The West Salton detachment fault was a coherent structure from the late Miocene (?) or Pliocene into the early Pleistocene based on stratigraphic relationships (Axen and Fletcher, 1998; Winker and Kidwell, 2002; Dorsey and Janecke, 2002; Kairouz, 2005; Dorsey, 2006; Dorsey et al., 2006; Lutz et al., 2006; Matti et al., 2006). A period of overlapping activity between the San Felipe fault zone and the West Salton detachment fault may be indicated by relationships along the Perpendicular Bluff fault, the N-striking splay of the San Felipe fault system described above. This sinistral-oblique fault offsets the main trace of the West Salton detachment in the south but does not cut a short, subsidiary strand of the detachment in the N that is localized within the footwall of the main detachment fault (Fig. 5). This relationship has been used as evidence for continued slip on the N-dipping part of the detachment fault after the S-dipping part was tilted southward and therefore deactivated, while the remainder of the detachment continued to slip. This geometry was interpreted as evidence for clockwise rotation of slip vectors on the West Salton detachment fault through time as the strain field evolved from transtension to dextral faulting (Axen et al., 2004). This "overlapping slip" model implies continued slip across the detachment N of Yaqui Ridge while the San Felipe fault was beginning to cut across it and deactivation of the SW-dipping part of the fault. The continued detachment slip on the NE side of Yaqui Ridge was then transferred eastward to another structure—presumably to the Sunset fault—for a period of time. The Sunset and Fish Creek Mountains faults are the only mapped structures available to accommodate slip from any still-active part of the detachment fault after deactivation in the south (Steely, 2006).

Both structural and stratigraphic lines of evidence make this overlapping slip model unattractive, though none completely rule it out: (1) The abrupt stratigraphic change from regional detachment-related subsidence (during deposition of the Borrego Formation) to localized basin subsidence and block uplift (during deposition of the Ocotillo Formation and erosion of the uplifted fault blocks along the San Felipe fault zone) occurred rapidly throughout the western Salton Trough at ca. 1.1 Ma (Lutz et al., 2006; Kirby et al., 2007). This result is not predicted if the detachment fault were still an active structure creating accommodation space on a regional scale. A gradual stratigraphic change from open lacustrine mud-dominated facies to basin-margin sand to gravel-dominated facies is expected in the San Felipe–Borrego basin, if there was coeval slip on the two structures. Instead the change is sharp and abrupt. (2) Strands of the San Felipe fault zone near Yaqui Ridge cut and offset the detachment fault 5.8 ± 2.8 km and show that this dextral fault zone is a younger crosscutting structure. Once the San Felipe fault cut the detachment on the south side of Yaqui Ridge, we infer that the detachment stopped slipping on both sides of the crossing fault. (3) The steep, SW-dipping reverse-dextral geometry of the Sunset fault nearest the gently NE-dipping West Salton detachment fault does not favor a transfer of strain between the two oppositely dipping faults. Furthermore, there is no overlap of slip directions between the detachment fault and the Sunset fault (Fig. 12), and we know of no evidence for strain partitioning because there is no suitable fault for partitioning nearby (Steely, 2006). (4) Initial top-to-the-NE slip across the West Salton detachment fault (Axen et al., 2004) is inconsistent with evidence for a large original corrugation in the West Salton detachment fault at Whale Peak. A corrugation there is required by the lack of an ESE-plunging fold in the hanging wall of the detachment that aligns with the corrugation and has the same strain as the foldlike form of the detachment fault (Kairouz, 2005). This major ESE-plunging antiformal corrugation is positioned in such a way as to preclude top-to-the-NE slip across the West Salton detachment fault at Whale Peak and Yaqui Ridge when it existed. (5) The overlapping slip model predicts that the detachment was active longer north of Yaqui Ridge than south of it, yet the opposite is true (Kairouz, 2005; Dorsey, 2008, written commun.). (6) Early Pleistocene deactivation of the West Salton detachment fault is also implied by the basinal studies of Johnson et al. (1983), Dorsey (2006), Lutz et al. (2006), and Kirby et al. (2007). (7) Finally, the relationship between the Perpendicular Bluff fault and the subsidiary detachment fault at Yaqui Ridge might be the result of the San Felipe fault zone reutilizing a short piece of a preexisting subsidiary detachment fault as it transforms the soft link in the Narrows stepover of the San Felipe fault zone into a hard link. Figure 5 shows this latter interpretation using color-coded faults.

The transition from Pliocene-age slip on the West Salton detachment fault to slip on new dextral-oblique faults was structurally complex and occurred at ca. 1.1 ± 0.2 Ma at Yaqui Ridge. Our data strongly suggest an abrupt change between the two fault systems, but may permit a more gradual change with at most a few hundred thousand years of overlapping activity. In any case, we infer that the West Salton detachment fault stopped being a major, regional structure in early Pleistocene time, by or before ca. 1.1 ± 0.2 Ma when the San Felipe fault zone initiated and cut across it. The West Salton detachment fault was certainly inactive by ca. 0.6 Ma.

Role of the San Felipe Fault in the San Andreas Fault System

The San Felipe fault zone is one of four dextral faults in southern California that together have accommodated roughly half of the motion across the San Andreas fault system since early Pleistocene time. The other half is taken up by the southern San Andreas fault itself (e.g., Fialko, 2006). The estimated 5.8 ± 2.8 km of right separation across the San Felipe fault zone near Yaqui Ridge on the San Felipe fault is greater than the right separation across the better known southern Elsinore fault (~2.5 km; Todd, 2004) and the Coyote Creek fault of the San Jacinto fault zone (~1–4 km; Janecke et al., 2005b; Steely, 2006). Because the San Felipe fault strikes toward the western Elsinore fault zone it may divert some of the slip from the NW third of the Elsinore fault zone onto other faults. This could help explain the apparent along-strike displacement gradient of the Elsinore fault zone (Magistrale and Rockwell, 1996). The San Jacinto fault zone dwarfs the San Felipe fault zone in its total right separation (19–29 km; Sharp, 1967; Hill, 1984) but the basinal effects of the San Felipe fault zone greatly exceeded those of the San Jacinto fault zone, perhaps because the San Felipe fault zone produced more vertical deformation (Fig. 11). All the data indicate nearly simultaneous initiation of the San Jacinto and San Felipe fault zones near the western margin of the Salton Trough in the early Pleistocene (Lutz et al., 2006; Steely, 2006; Kirby et al., 2007; this study). This reorganization represents a major transition from transtension localized on two major faults to distributed dextral faulting in a wide complex zone comprised of at least four dextral fault zones. Other data sets show that the transition also results in widespread transpression south of the Big Bend (Janecke and Belgarde, 2007).

CONCLUSIONS

The San Felipe fault zone initiated in Pleistocene time and is part of a relatively new geometry of the larger San Andreas fault system.

We date its inception to the early Pleistocene, when it cut, folded, and deactivated the West Salton detachment fault in a restraining bend and contractional stepover near Yaqui Ridge. The San Felipe fault zone propagated to the surface at ca. 1.1 ± 0.2 Ma, may have initiated in the subsurface slightly before then, and is therefore coeval with the adjacent San Jacinto and Elsinore faults. It is not an older dextral fault as some previous workers suggested. The San Felipe fault zone accumulated up to 5.8 ± 2.8 km of right slip, and continues to be active in late Pleistocene to Holocene time. Near Yaqui Ridge the fault zone consists of the left-stepping, en echelon, San Felipe, Sunset, and Fish Creek Mountains faults at the E end of an ~15-km-long, E-W–striking restraining bend. Overall the fault steps ~9 km to the left by bending and stepping near Yaqui Ridge. The dextral-oblique Sunset fault is in the middle of this complex left stepover and bend, and controlled deposition of the Pleistocene Sunset Conglomerate of the Ocotillo Formation. Deactivation of the West Salton detachment fault near Yaqui Ridge probably occurred rapidly as the southernmost San Andreas fault system changed from a partially transtensional mode to a wrench and dextral mode of deformation.

The Sunset Conglomerate consists of angular boulder conglomerate to conglomeratic coarse sandstone, was deposited in alluvial fans with NE transport, coarsens up and toward the basin-bounding Sunset fault, and contains recycled sandstone clasts from exhumed Pliocene basin fill. The appearance of recycled clasts in the Ocotillo Formation throughout the SW Salton Trough records uplift and stripping of older basin fill from the paleo-Vallecito and Fish Creek Mountains. Initiation of the San Felipe fault zone had a major impact on the supradetachment basin above the older West Salton detachment fault, and separated it into the Vallecito–Fish Creek subbasin in the south and the San Felipe–Borrego subbasin in the north. The San Jacinto fault zone produced more subtle basinal changes at roughly the same time (Lutz et al., 2006; Kirby et al., 2007).

The San Felipe fault zone is little more than 1 m.y. old near Yaqui Ridge, yet it has already experienced major topographic inversions and kinematic and geometric changes. We currently identify three stages of fault growth and deformation. An initial, broad, fault-propagation monocline faced NE during the blind upward growth of the tip of the Sunset and Fish Creek Mountains faults ca. 1.1–1.3 Ma. A SW-facing monocline probably initiated at about the same time NE of the San Felipe fault and ultimately produced the Yaqui Ridge antiform. The first phase of deformation began to disrupt slip across the West Salton detachment fault, eroded some of the Borrego or Hueso Formation that may have been present in the Vallecito Mountains, and tilted Pliocene sedimentary rocks ~10°–15° to the NE. The second phase began at ca. 1.1 ± 0.2 Ma when three left-stepping faults of the San Felipe fault zone breached the surface. This initiated deposition of the Sunset Conglomerate of the Ocotillo Formation NE of the Sunset dextral-oblique fault, and resulted in rapid progradation of conglomerate and pebbly sandstone throughout the newly subdivided San Felipe–Borrego basin. A NE-down component of slip on the Sunset and Fish Creek Mountains faults produced >600 m of accommodation space for the Sunset Conglomerate of the Ocotillo Formation. During the third and current phase of deformation, which started roughly 0.5–0.6 Ma, NE-SW shortening continues, and former areas of subsidence and sediment accumulation are being inverted and exhumed within the fault zone.

ACKNOWLEDGMENTS

Thanks to R. Crippen, R. Blom, and T. Rockwell for merged Landsat and SPOT data of the area. This research was supported by grants from the National Science Foundation (to S.U. Janecke, R.J. Dorsey, and G.J. Axen) and Petroleum Research Fund of the American Chemical Society (S.U. Janecke). G. Jefferson and the staff of the Anza-Borrego Desert State Park kindly housed our field crews and provided logistical support. Rick Allmendinger's stereonet program was essential for analysis and plotting. This research benefited from insightful discussions with J. Evans, B. Housen, G. Jefferson, S. Kirby, A. Lutz, B. Belgarde, T. Rockwell, and R. Weldon. Thorough reviews by Victoria Langenheim, Jonathon Nourse, Walter Sullivan, and two anonymous reviewers improved the final version of the paper.

REFERENCES CITED

Atwater, T., 1970, Implications of plate tectonics for the Cenozoic evolution of western North America: Geological Society of America Bulletin, v. 81, p. 3513–3536, doi: 10.1130/0016-7606(1970)81[3513:IOPTFT]2.0.CO;2.

Axen, G.J., and Fletcher, J.M., 1998, Late Miocene-Pleistocene extensional faulting, Northern Gulf of California, Mexico and Salton Trough, California: International Geology Review, v. 40, p. 217–244.

Axen, G., Kairouz, M., Steely, A.N., Janecke, S.U., and Dorsey, D.J., 2004, Structural expressions of low-angle faults developed in wrench settings: An example from the West Salton detachment fault system: Geological Society of America Abstracts with Programs, v. 36, p. 548.

Bartholomew, M.J., 1968, Geology of the northern portion of Seventeen Palms and Font's Point quadrangles, Imperial and San Diego Counties, California [M.S. thesis]: Los Angeles, University of Southern California, 60 p.

Belgarde, B.E., 2007, Structural characterization of the three SE segments of the Clark fault, Salton Trough, California [M.S. thesis]: Utah State University, 4 plates, map scale 1:24,000, 216 p.

Bennett, R.A., Rodi, W., and Reilinger, R.E., 1996, GPS constraints on fault slip rates in southern California and northern Baja, Mexico: Journal of Geophysical Research, v. 101, no. B10, p. 21,943–21,960, doi: 10.1029/96JB02488.

Brown, N., Fuller, M.D., and Sibson, R.H., 1991, Paleomagnetism of the Ocotillo Badlands, southern California, and implications for slip transfer through an antidilational fault jog: Earth and Planetary Science Letters, v. 102, p. 277–288, doi: 10.1016/0012-821X(91)90023-B.

Crowell, J.C., 1981, An outline of the tectonic history of southeastern California, *in* Ernst, W.G., ed., The geotectonic development of California: Englewood Cliffs, New Jersey, Prentice-Hall, Rubey Volume I, p. 583–600.

Dibblee, T.W., Jr., 1954, Geology of the Imperial Valley Region, California: Geology of southern California: California Division of Mines Bulletin, v. 170, p. 21–28.

Dibblee, T.W., Jr., 1984, Stratigraphy and tectonics of the San Felipe Hills, Borrego Badlands, Superstition Hills, and vicinity, *in* Rigsby, C.A., ed., 1984, The Imperial Basin-tectonics, sedimentation, and thermal aspects: Society for Sedimentary Geology (SEPM), Pacific Section, p. 31–44.

Dibblee, T.W., Jr., 1996, Stratigraphy and tectonics of the Vallecito-Fish Creek Mountains, Vallecito Badlands, Coyote Mountain, and Yuha Desert, southwestern Imperial basin, *in* Abbott, P.L. and Seymour, D.C., eds., 1996, Sturtzstroms and detachment faults, Anza-Borrego Desert State Park, California. South Coast Geological Society Annual Field Trip Guide Book, no. 24, p. 59–79.

Dorsey, R.J., 2002, Stratigraphic record of Pleistocene initiation and slip on the Coyote Creek fault, lower Coyote Creek, Southern California, *in* Barth, A., ed., Contributions to crustal evolution of the southwest United States: Boulder, Colorado, Geological Society of America Special Paper 365, p. 251–269.

Dorsey, R.J., 2006, Stratigraphy, tectonics, and basin evolution in the Anza-Borrego Desert region, *in* Jefferson, G.T., and Lindsay, L.E. eds., Fossil treasures of Anza-Borrego Desert: San Diego, California, Sunbelt Publications, p. 89–104.

Dorsey, R.J., and Janecke, S.U., 2002, Late Miocene to Pleistocene West Salton detachment fault system and basin evolution, southern California: New insights: Geological Society of America Abstracts with Programs, v. 34, no. 6, p. 248.

Dorsey, R.J., Janecke, S.U., Kirby, S.M., McDougall, K.A., and Steely, A.N., 2005, Pliocene evolution of the lower Colorado River in the Salton Trough: Tectonic controls on regional paleogeography and the regional Borrego Lake, *in* Reheis, M.C., ed., Geologic and biotic perspectives on late Cenozoic drainage history of the southwestern Great Basin and lower Colorado River region: Conference Abstracts: U.S. Geological Survey Open-File Report 2005-1404, p. 13.

Dorsey, R. J., Fluette, A., McDougall. K. A., Housen, B. A., Janecke, S. U., Axen, G. A., and Shirvell, C. R., 2007, Chronology of Miocene-Pliocene deposits at Split Mountain Gorge, southern California: A record of regional tectonics and Colorado River evolution: Geology, v. 35, p. 57–60.

Dorsey, R. J., Fluette, A. L., Housen, B. A., McDougall, K. A., Janecke, S. U., Axen, G. J., and Shirvell, C., 2006, Chronology of Late Miocene to Early Pliocene Sedimentation at Split Mt. Gorge, Western Salton Trough: Implications for Development of the Pacific-North America Plate: Abstracts for NSF MARGINS program, Workshop on Rupturing of Continental Lithosphere: Ensenada Mexico, January 9-13, p. 23–24: http://rclcortez.wustl.edu/Workshop_Abstracts.pdf.

Fialko, Y., 2006, Interseismic strain accumulation and the earthquake potential on the southern San Andreas fault system: Nature, v. 441, p. 968–971, doi: 10.1038/nature04797.

Gawthorpe, R.L., Sharp, I., Underhill, J., and Gupta, S., 1997, Linked sequence stratigraphic and structural evolution of propagating normal faults: Geology, v. 25, p. 795–798, doi: 10.1130/0091-7613(1997)025<0795:LSSASE>2.3.CO;2.

Hill, R.I., 1984, Petrology and petrogenesis of batholithic rocks, San Jacinto Mountains, southern California [Ph.D. thesis]: Pasadena, California Institute of Technology, 800 p.

Housen, B.A., Dorsey, R.J., Janecke, S.U., and Axen, G.J., 2005, Rotation of Plio-Pleistocene sedimentary rocks in the Fish Creek Vallecito Basin, western Salton Trough, California: Eos (Transactions, American Geophysical Union), v. 86, #GP13A–0039.

Hull, A.G., and Nicholson, C., 1992, Seismotectonics of the northern Elsinore fault zone, Southern California: Bulletin of the Seismological Society of America, v. 82, no. 2, p. 800–818.

Janecke, S.U., and Belgarde, B.E., 2007, The width of dextral fault zones and shallow décollements of the San Jacinto fault zone, southern California: Palm Springs, California, Annual Meeting of the Southern California Earthquake Center, v. 17. http://www.scec.org/meetings/2007am/index.html

Janecke, S.U., Vandenburg, C.J., and Blankenau, J.J., 1998, Geometry, mechanisms and significance of extensional folds from examples in the Rocky Mountain Basin and Range Province, U.S.A: Journal of Structural Geology, v. 20, p. 841–856, doi: 10.1016/S0191-8141(98)00016-9.

Janecke, S.U., Dorsey, R.J., Kickham, J.C., Matoush, J.P., and McIntosh, W., 2005a, Geologic map of the Bachelor Mountain Quadrangle, southwest Montana: Montana Bureau of Mines Open-File Report 525, scale 1:24,000, 28 p.

Janecke, S.U., Kirby, S.M., Langenheim, V., Steely, A.N., Dorsey, R., Housen, B., and Lutz, A., 2005b, High geologic slip rates on the San Jacinto fault zone in the SW Salton Trough, and possible near-surface slip deficit in sedimentary basins: Geological Society of America Abstracts with Programs, v. 37, no. 7, p. 275.

Jennings, C.W., 1977, Geologic map of California: Sacramento, California, California Division of Mines and Geology, scale 1:750,000.

Johnson, M., Officer, C.B., Opdyke, D., Woodard, G.D., Zeitler, P.K., and Lindsay, E.H., 1983, Rates of late Cenozoic tectonism in the Vallecito-Fish Creek basin, western Imperial Valley, California: Geology, v. 11, p. 664–667, doi: 10.1130/0091-7613(1983)11<664:ROLCTI>2.0.CO;2.

Kairouz, M.E., 2005, Geology of the Whale Peak Region of the Vallecito Mountains: Emphasis on the kinematics and timing of the West Salton detachment fault, southern California [M.S. thesis]: Los Angeles, University of California, 56 p.

Kendrick, K.J., Morton, D.M., Wells, S.G., and Simpson, R.W., 2002, Spatial and temporal deformation along the northern San Jacinto Fault, southern California: Implications for slip rates (*in* Paleoseismology of the San Andreas fault system): Bulletin of the Seismological Society of America, v. 92, no. 7, p. 2782–2802.

Kennedy, M.P., and Morton, D.M., 2003, Preliminary geologic map of the Murrieta 7.5′ quadrangle, Riverside County, California: U.S. Geological Survey Open-File Report 03-189.

King, T., Cox, B.F., Matti, J.C., Powell, C.L., II, Osterman, L.E., and Bybell, L.M., 2002, Previously unreported outcrops of Neogene Imperial Formation in southern Santa Rosa Mountains, California, and implications for tectonic uplift: Geological Society of America Abstracts with Programs, v. 34, p. 124.

Kirby, S.M., 2005, The Quaternary tectonic and structural evolution of the San Felipe Hills, California [M.S. thesis]: Logan, Utah State University, 182 p.

Kirby, S.M., Janecke, S.U., Dorsey, R.J., Housen, B.A., McDougall, K., Langenheim, V., and Steely, A., 2007, Pleistocene Brawley and Ocotillo Formations: Evidence for initial strike-slip deformation along the San Felipe and San Jacinto fault zones, California: The Journal of Geology, v. 115, no. 1, p. 43–62, doi: 10.1086/509248.

Lamar, D.L., and Rockwell, T.K., 1986, An overview of the tectonics of the Elsinore fault zone, *in* Ehlig, P., ed., Guidebook and volume on neotectonics and faulting in southern California, Cordilleran Section: Geological Society of America, p. 149–158.

Lough, C.F., 1993, Structural evolution of the Vallecito Mountains, Colorado Desert and Salton Trough Geology: San Diego, California, San Diego Association of Geologists, p. 91–109.

Lutz, A.T., 2005, Tectonic controls on Pleistocene basin evolution in the central San Jacinto fault zone, southern California [M.S. thesis]: Eugene, University of Oregon, 136 p.

Lutz, A.T., Dorsey, R.J., Housen, B.A., and Janecke, S.U., 2006, Stratigraphic record of Pleistocene faulting and basin evolution in the Borrego Badlands, San Jacinto fault zone, Southern California: Geological Society of America Bulletin, v. 118, no. 11, p. 1377–1397, doi: 10.1130/B25946.1

Magistrale, H., and Rockwell, T., 1996, The central and southern Elsinore fault zone, southern California: Bulletin of the Seismological Society of America, v. 861, p. 791–803.

Matti, J.C., and Morton, D.M., 1993, Paleogeographic evolution of the San Andreas fault in southern California: A reconstruction based on a new cross fault correlation, *in* Powell, R.E., et al., eds., The San Andreas fault system: Displacement, palinspastic reconstruction, and geologic evolution: Geological Society of America Memoir 178, p. 107–159.

Matti, J.C., Morton, D.M., Cox, B.F., Landis, G.P., Langenheim, V.E., Premo, W.R., Kistler, R., and Budahn, J.R., 2006, Fault bounded late Neogene sedimentary deposits in the Santa Rosa Mountains, southern California: Constraints on the evolution of the San Jacinto fault: Eos (Transactions, American Geophysical Union), v. 87, no. 52, T21B-0407.

Merriam, R., and Bandy, O.L., 1965, Source of upper Cenozoic sediments in the Colorado delta region: Journal of Sedimentary Petrology, v. 35, p. 911–916.

Morley, E.R., 1963, Geology of the Borrego Mountain quadrangle and the western portion of the Shell Reef quadrangle, San Diego County, California [M.S. thesis]: Los Angeles, University of Southern California, 138 p.

Morton, D.M., and Matti, J.C., 1993, Extension and contraction in an evolving divergent strike-slip fault complex: The San Andreas and San Jacinto fault zones at their convergence in Southern California, *in* Powell, R.E., Weldon, R.J., and Matti, J.C., eds., The San Andreas fault system: Displacement, palinspastic reconstruction, and geologic evolution: Geological Society of America Memoir, v. 178, p. 217–230.

Reitz, D.T., 1977, Geology of the western and central San Felipe Hills, northwestern Imperial County, California [M.S. thesis]: Los Angeles, University of Southern California, 155 p.

Rockwell, T., Loughman, C., and Merifield, P., 1990, Late Quaternary rate of slip along the San Jacinto fault zone near Anza, Southern California: Journal of Geophysical Research, v. 95, p. 8593–8605, doi: 10.1029/JB095iB06p08593.

Rogers, T.H., 1965, Santa Ana sheet: California Division of Mines and Geology Geologic Map of California, scale, 1:250,000.

Sanders, C.O., 1989. Fault segmentation and earthquake occurrence in the strike-slip San Jacinto fault zone, California, *in* Schwartz, D.P., and Sibson, R.H., eds., Proceedings of Conference XLV: A workshop on fault segmentation and controls of rupture initiation and termination: U.S. Geological Survey Open-File Report OF 89-0315, p. 324–349.

Schultejann, P.A., 1984, The Yaqui Ridge antiform and detachment fault: Mid-Cenozoic extensional terrane west of the San Andreas fault: Tectonics, v. 3, no. 6, p. 677–691, doi: 10.1029/TC003i006p00677.

Sharp, I., Gawthorpe, R.L., Underhill, J., and Gupta, S., 2000, Fault propagation folding in extensional settings: Examples of structural style and synrift sedimentary response from the Suez Rift, Sinai, Egypt: Geological Society of America Bulletin, v. 112, no. 12, p. 1877–1899, doi: 10.1130/0016-7606(2000)112<1877:FPFIES>2.0.CO;2.

Sharp, R.V., 1967, San Jacinto fault zone in the Peninsular Ranges of southern California: Geological Society of America Bulletin, v. 78, p. 705–730, doi: 10.1130/0016-7606(1967)78[705:SJFZIT]2.0.CO;2.

Sharp, R.V., 1972, Tectonic setting of the Salton Trough, *in* Sharp, R.V., ed., The Borrego Mountain earthquake of April 9, 1968: U.S. Geological Survey Professional Paper, p. 15.

Steely, A.N., Janecke, S.U., Dorsey, R.J., and Axen, G.J., 2004, Evidence for Late Miocene-Quaternary low-angle oblique strike-slip faulting on the West Salton detachment fault, southern California: Geological Society of America Abstracts with Program, v. 36, no. 4, p. 37.

Steely, A.N., 2006, The evolution from late Miocene West Salton detachment faulting to cross-cutting oblique strike-slip faults in the SW Salton Trough, California [M.S. thesis]: Utah State University, 253 p., 3 plates, scale 1:24,000.

Stinson, A.L., and Gastil, R.G., 1996, Mid- to Late-Tertiary detachment faulting in the Pinyon Mountains, San Diego County, California: A setting for long run-out landslides in the Split Mountain Gorge area, *in* Abbott, P.L., and Seymour, D.C., eds., Sturtzstroms and detachment faults, Anza-Borrego Desert State Park, California: Santa Ana, California, South Coast Geological Society, p. 221–244.

Tarbet, L.A., and Holman, W.H., 1944, Stratigraphy and micropaleontology of the west side of the Imperial Valley, California: American Association of Petroleum Geologists Abstracts, v. 28, p. 1781–1782.

Todd, V.R., 2004, Preliminary geologic map of the El Cajon 30′ × 60′ quadrangle, southern California: U.S. Geological Survey Open-File Report 2004-1361, scale 1:100,000, 30 p.

Todd, V.R., Erskine, B.E., and Morton, D.M., 1988, Metamorphic and tectonic evolution of the northern Peninsular Ranges batholith, southern California, *in* Ernst, W.G., ed., Metamorphism and crustal evolution of the western United States (Rubey Volume VII): Englewood Cliffs, New Jersey, Prentice-Hall, p. 894–937.

Wagner, D.L., 1996, Geologic map of the Tubb Canyon 7.5. quadrangle, San Diego County, California: California Division of Mines and Geology Open-File Report 96-06.

Winker, C.D., 1987. Neogene stratigraphy of the Fish Creek-Vallecito section, southern California: Implications for early history of the northern Gulf of California and Colorado delta [Ph.D. thesis]: Tucson, University of Arizona, 494 p.

Winker, C.D., and Kidwell, S.M., 1986, Paleocurrent evidence for lateral displacement of the Colorado River delta by the San Andreas fault system, southeastern California: Geology, v. 14, p. 788–791, doi: 10.1130/0091-7613(1986)14<788:PEFLDO>2.0.CO;2.

Winker, C.D., and Kidwell, S.M., 1996, Stratigraphy of a marine rift basin: Neogene of the western Salton Trough, California, *in* Abbott, P.L., and Cooper, J.D., eds., Field conference guidebook and volume for the annual convention: San Diego, California, American Association of Petroleum Geologists, Pacific Section, p. 295–336.

Winker, C.D., and Kidwell, S.M., 2002, Stratigraphic evidence for ages of different extensional styles in the Salton Trough, southern California: Geological Society of America Abstracts with Programs, v. 34, no. 6, p. 884.

Manuscript Received 2 April 2007
Revised Manuscript Received 7 May 2008
Manuscript Accepted 27 May 2008

Printed in the USA